Electronic Supplementary Material (ESI) for Molecular Systems Design & Engineering.

Supporting Information

Machine Learning Assisted Identifying the Matched Energy Level of Material for High Open Circuit Voltage in Binary Organic Solar Cells

Kuo Wang[a], Chaorong Guo[a], Zhennan Li[a], Rui Zhang[a], Zhimin Feng[a], Gengkun Fang[a], Di Huang[a,*], Jiaojiao Liang[a,b*], Ling Zhao[c,*], Zicha Li[d]

a, *Hunan University of Technology, College of Railway Transportation, Zhuzhou 412008, China*

b, *Qinghai Provincial Key Laboratory of Nanomaterials and Nanotechnology, Qinghai Minzu University, Qinghai 810007, China*

c, *Shandong Provinical Key Laboratory of Optical Communication Science and Technology, School of Physical Science and Information Technology, Liaocheng University, Liaocheng 252059, China*

d, *Key Laboratory of Optical Information Detecting and Display Technology, Zhejiang Normal University, Jinhua 321004, China*

*Corresponding author: dihuang@hut.edu.cn, liangjiaojiao@hut.edu.cn, zhaoling9966@163.com

Experimental details:

Dataset collection: 400 groups of devices' V_{oc} data points along with the materials' energy level directly obtain from 106 publications reported in various journals since 2015, which are applied as the available datasets in the bellowed file to analyze the potential relationship between the energy level of materials and V_{oc} in OSCs.[1-106] The datasets contains six input feature variables (the work function of hole transport layer (WFs-HTL), the work function of electron transport layer (WFs-ETL), HOMO and LUMO of the donor ($HOMO_{(D)}$ and $LUMO_{(D)}$), HOMO and LUMO of the acceptor ($HOMO_{(A)}$ and $LUMO_{(A)}$) and one output characteristic parameter (V_{oc}). In most of these studies, ultraviolet photoemission spectroscopy (UPS) is used to measure the HOMO energy level of the film. The LUMO energy level of the film was characterized by inverse photoelectron spectroscopy (IPES). In the dataset, KNN algorithm is used to fill in very few missing values. Meanwhile, the dataset is randomly divided into two parts: training set (80% of dataset) for model training and testing set (20% of database) for data prediction. In small datasets, the distribution of training and testing segmentation usually change. Therefore, the dataset is randomly shuffled for many times and the average value is adopted to further ensure the reliability of learning model prediction.[107]

See "**Table S1.** Dataset of Machine Learning" for details in the below.

Model building: In this work, learning models are built based on the Python language environment. And four type of algorithms (K-Nearest Neighbor (KNN), Support Vector Regression

(SVR), Random Forest (RF) and eXtreme Gradient Boosting (XGBoost)) are used to evaluate the performance of model prediction. Among them, the KNN algorithm is a kind of non-parametric statistical lazy algorithm. For predicting the target value, the average of the K nearest values is assigned. In other words, the similar inputs have the similar outputs. The SVR algorithm is to solve the regression problem by fitting the training sample points on the hyperplane with a certain "tolerance limitation", which obtain the optimized model by minimizing the loss and maximizing the interval. RF algorithm is a very representative bagging ensemble algorithm. All of the base evaluators are decision trees. Based on the random sampling of bagging samples, random selection of features is added in RF. In this report, every given predicted V_{oc} result from the RF algorithm is average value by the base estimator.[108,109] XGBoost algorithm is built by the parallel construction of regression trees through multi-threading, which can control the model during the entire training process through a series of hyperparameters to greatly improve the speed and accuracy of model training.[110,111] The RF model and the XGBoost model fit relatively well among the four used ML algorithms in this work. And Both of them belong to the tree-based ML algorithms, which can provide good overall performance in prediction models because they reflect the made decisions by the vast majority of trees.

What's more, the python code is used to calculate the Pearson correlation coefficient, as follows:

```
# Prepare some needed libraries
import pandas as pd
import seaborn as sns
import matplotlib.pyplot as plt
from pandas import read_csv
from matplotlib.pyplot import savefig
# Read and fit data
filename = 'BOSCs.csv'
# names = ['WFs-HTL', 'WFs-ETL', 'HOMO(D)', 'LUMO(D)', 'HOMO(A)', 'LUMO(A)', 'Voc', 'Jsc', 'FF', 'PCE']
data = read_csv(filename)
ad = data.iloc[:, 5:11]
print(ad, type(ad))
voc = data.iloc[:, column]
jsc = data.iloc[:, column]
pce = data.iloc[:, column]
ad_voc0 = pd.concat([ad, voc], axis=1)
ad_voc1 = pd.concat([ad, jsc], axis=1)
```

```
ad_voc2 = pd.concat([ad, pce], axis=1)
ad_voc3 = ad_voc0.corr()
ad_voc4 = ad_voc1.corr()
ad_voc5 = ad_voc2.corr()
# Plot
plt.subplots(figsize=(8, 8))
sns.heatmap(ad_pce3/4/5, annot=True, vmin=-0.6, vmax=1, square=True, cmap="Greens")
savefig(" .jpg")
plt.show()
```

Performance evaluation: As shown in Equations (1), (2) and (3), the coefficient of determination (R^2), root mean square error (RMSE) and mean absolute error (MAE) are often used to evaluate algorithms with regression problems:

$R^2 = \frac{\left[\sum_{i=1}^{n}(y_i' - \hat{y})(y_i' - \hat{y}')\right]^2}{\sum_{i=1}^{n}(y_i - \hat{y})^2 \cdot \sum_{i=1}^{n}(y_i' - \hat{y}')^2}$	（1）
$RMSE = \sqrt{\frac{\sum_{i=1}^{n}(y_i' - y_i)^2}{n}}$	（2）
$MAE = \frac{1}{m}\sum_{i=1}^{m}\lvert(y_i - \hat{y}_i)\rvert$	（3）

Where n is the total number of data, y_i and y_i' represent the tested and predicted values, ˆ y and ˆ y' are the average values of the tested and predicted values, respectively.

Pearson correlation coefficient is also called the linear correlation coefficient, which is used to detect the degree of linear correlation between two continuous variables. The calculation formula (4) of the Pearson correlation coefficient of the sample is as follows:

$r_{xy} = \frac{n\sum x_i y_i - \sum x_i \sum y_i}{\sqrt{n\sum x_i^2 - \left(\sum x_i\right)^2} \cdot \sqrt{n\sum y_i^2 - \left(\sum y_i\right)^2}}$	（4）

Where, n represents the number of observation objects, x_i and y_i represent the i-th observation of x and y, respectively. It is clear that r stand for the quotient of the covariance and the standard deviation between two variables.

Devices fabrication: PTB7, PTB7-Th, PffBT4T-2OD were from 1Materials, $PC_{71}BM$ was from Nano-C, and PM6, Y6, ITIC-M were purchased from Solarmer Materials Inc. Chlorobenzene (CB) and 1,8-diiodooctane (DIO) were commercially procured from J&K Scientific and Alfa Aesar with over 99.9% and 99.8% purity, respectively. All materials were purchased from suppliers and can be used without further processing. The ITO glass substrates were ultrasonically treated in special glass lotion, deionized water and ethanol for 20min in each step, respectively. And then air-dried with high-purity nitrogen. The pre-cleaned ITO were treated with ultraviolet ozone for 5min to improve the work function of ITO. Then PEDOT:PSS was spin-coated on ITO substrate for 50s at 4000rpm/min, annealed at 150℃ for 15min in air, after that, the substrate was transferred to the glove box for later using. The MoOx layer was thermally evaporated onto the substrate at a rate of 0.5 Å/s under a vacuum of less than $3*10^{-4}$ Pa with 8nm thickness. The normal device structure is ITO/HTLs/Active Layer/ETLs/Ag.

Devices with $PC_{71}BM$: The PTB7:$PC_{71}BM$, PTB7-Th:$PC_{71}BM$ blended solutions (concentration is 20mg/ml and weight ratio is 1:1.5) were prepared and added 3v% DIO as additive by dissolving in CB, respectively. And the blended solutions were stirred for one day before use. The active layer film was prepared by spin coating at 1000rpm for 1min. For PffBT4T-2OD:$PC_{71}BM$ film, the weight ratio of was 1:1.3 and the total concentration of blend solution is 32.2mg/ml, Then PffBT4T-2OD:$PC_{71}BM$ solutions were stirred overnight at 110℃ and spin-cast with 1000rpm for 25s onto the warm substrates which were heated by the 110℃ heating platform, and the substrate with PffBT4T-2OD:$PC_{71}BM$ film were annealed at 80℃ for 10min. LiF with a thickness of 8Å was deposited as the interface layer under the vacuum condition of $1*10^{-4}$ Pa. Finally, 100 nm Ag was deposited on the LiF as the top electrode and completed the device fabricating.

Devices with PM6: The PM6:Y6 and PM6:ITIC-M blended solutions (concentration 20mg/ml, weight ratio 1:1.2) were prepared by dissolving in CB respectively and added 0.5v% DIO as additive, the solution is heated and stirred at 45℃ for 3h. The active layer was prepared by spin coating at 3000rpm/min for 30s. The substrates with the active layer was annealed at 100℃ for 10min. PDINO was mixed with 1mg/ml methanol solution and spin-coated on the top of the active layer at 3000rpm/min for 50s. Finally, 100 nm Ag was deposited on PDINO as the top electrode and completed the device fabricating. The area of device is $4mm^2$, which is decided by the overlap area between Ag and ITO.

For the inverted device structure is ITO/ZnO/Active Layer/MoOx/Ag. The ZnO nanoparticle solution (2.5 wt%) was diluted in IPA at a ratio of 1:1, spin-coated on ITO substrate at 5000rpm for 40s, then annealed at 85℃ for 10min in air, cooled to room temperature and transferred to glove box for using. The PTB7:$PC_{71}BM$ mixed solution was spin cast at 1000rpm for 1min on the substrate.

MoOx is deposited as the interface layer under the vacuum condition of 1*10^{-4} Pa, and 100 nm Ag is deposited as the electrode to complete the device fabrication.

Devices measurement: The current-voltage (J-V) characteristics were tested by a Keithley 2400 Source Meter under simulated solar light (100 mW/cm^2, AM 1.5G, Abet Solar Simulator Sun2000).

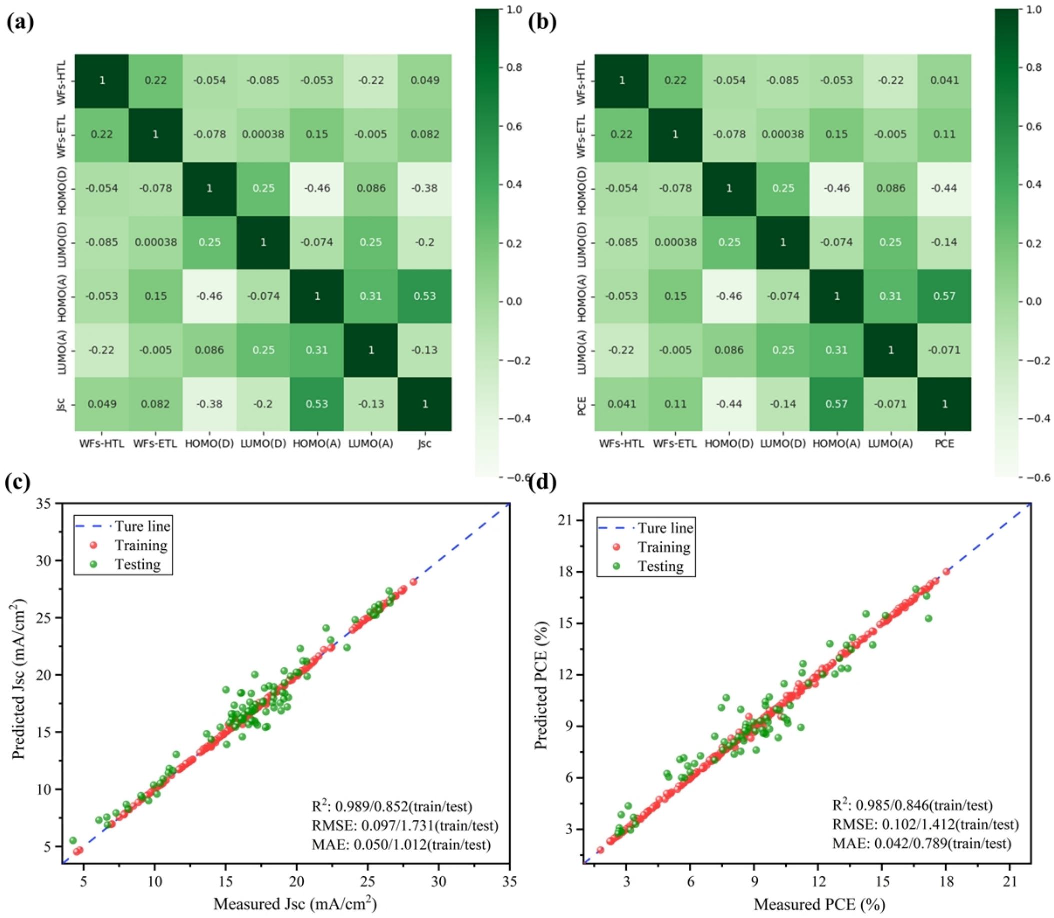

Figure S1. (a) Correlation matrix between J_{sc} and input features, (b) Correlation matrix between PCE and input features, (c) Correlation regression of the XGBoost model with the predicted J_{sc} and measured J_{sc}, (d) Correlation regression of the XGBoost model with the predicted PCE and measured PCE.

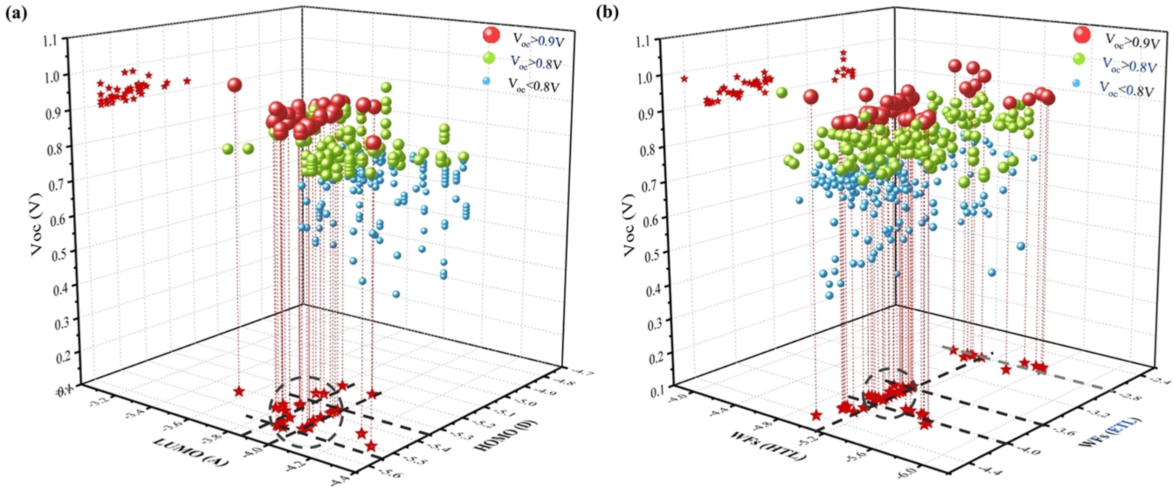

Figure S2. (a) The scattering interval described by V_{oc} as a function of $HOMO_{(D)}$ and $LUMO_{(A)}$, (b) Scattering interval described by V_{oc} as a function of WFs-ETL and WFs-HTL. (The red star in the figure indicates the scattering interval of V_{oc} with over 0.9V)

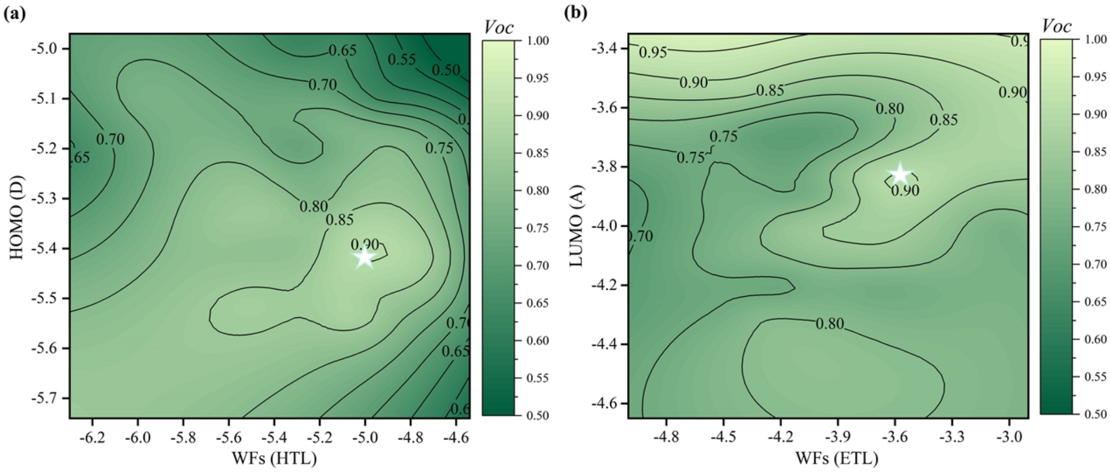

Figure S3. (a) The contour plot of predicted V_{oc} depends on $HOMO_{(D)}$ and $WFs_{(HTL)}$, (b) The contour plot of predicted V_{oc} depends on $LUMO_{(A)}$ and $WFs_{(ETL)}$.

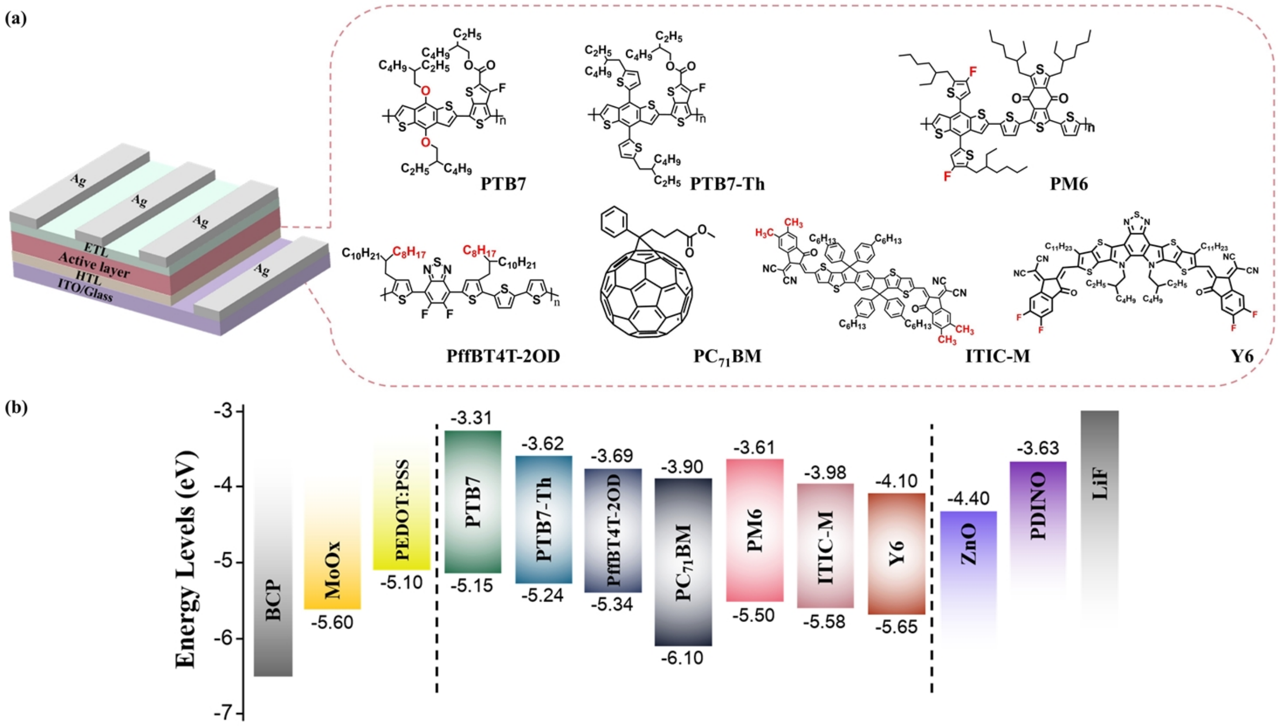

Figure S4. (a) The device structure and materials chemical structure of OSCs in this work, (b) Schematic diagram of energy level structure for each material.

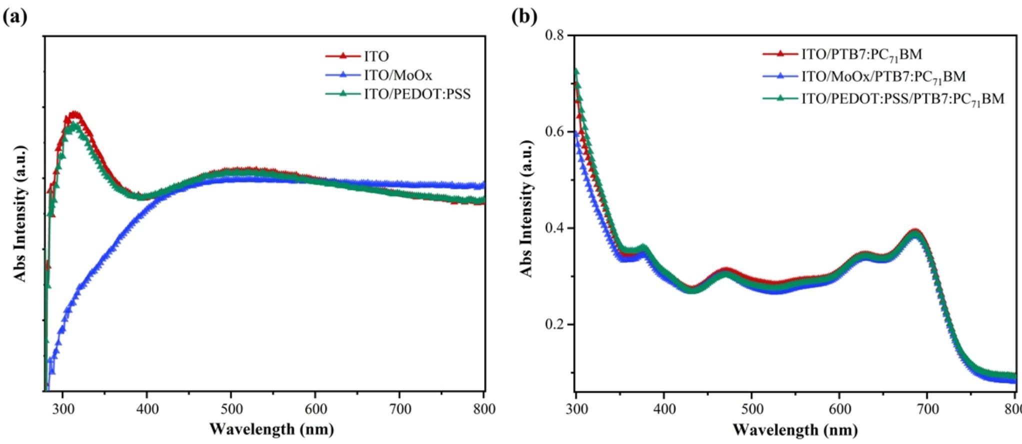

Figure S5. (a) Transmission spectra of different hole transport layer on ITO substrate and (b) Absorption spectra PTB7:$PC_{71}BM$ films on ITO substrate with the different hole transport layer.

Table S1. The dataset: Experimentally measured Energy Levels and Work Functions ($HOMO_{(D)}$ and $LUMO_{(D)}$ of Donors, $HOMO_{(A)}$ and $LUMO_{(A)}$ of Acceptors, Work Functions of Hole transport materials and Electron transport materials) and Device performance parameters (V_{oc}, J_{sc}, FF, PCE)

HTL	ETL	WFs-HTL	WFs-ETL	Active Layer	Donor	$HOMO_{(D)}$	$LUMO_{(D)}$	Acceptor	$HOMO_{(A)}$	$LUMO_{(A)}$	V_{oc}	J_{sc}	FF	PCE	Class	Year	Ref	$\|HOMO_{(D)}-LUMO_{(A)}\|$	$HOMO_{(I)}$	$LUMO_{(I)}$
PEDOT:PSS	PFN-Br	-5.10	-2.80	PBDB-T:ITIC	PBDB-T	-5.33	-2.92	ITIC	-5.51	-3.78	0.890	16.28	71.00	10.20	1	201	1	1.55	0.18	0.86
PEDOT:PDAS	PFN-Br	-5.38	-2.80	PBDB-T:ITIC	PBDB-T	-5.33	-2.92	ITIC	-5.51	-3.78	0.890	15.85	72.00	9.75	1	201	1	1.55	0.18	0.86
MoO3	Em-Ag/AgNWs:AZO-	-5.30	-4.31	PBDB-T-2F:Y6	PBDB-T-2F	-5.50	-3.56	Y6	-5.65	-4.10	0.832	25.05	72.97	15.21	1	202	2	1.40	0.15	0.54
MoO3	Em-Ag/AgNWs:AZO	-5.30	-4.28	PBDB-T-2F:Y6	PBDB-T-2F	-5.50	-3.56	Y6	-5.65	-4.10	0.826	21.90	67.38	12.19	1	202	2	1.40	0.15	0.54
PCP-2F-Li	PFN-Br	-4.99	-2.80	PBDBT-2F:IT-4F	PBDBT-2F	-5.54	-3.65	IT-4F	-5.66	-4.14	0.840	20.40	73.00	12.70	1	201	3	1.40	0.12	0.49
PCP-2F-Na	PFN-Br	-4.97	-2.80	PBDBT-2F:IT-4F	PBDBT-2F	-5.54	-3.65	IT-4F	-5.66	-4.14	0.810	19.50	72.00	11.80	1	201	3	1.40	0.12	0.49
PCP-Li	PFN-Br	-4.93	-2.80	PBDBT-2F:IT-4F	PBDBT-2F	-5.54	-3.65	IT-4F	-5.66	-4.14	0.780	18.50	71.00	10.70	0	201	3	1.40	0.12	0.49
PCP-Na	PFN-Br	-4.83	-2.80	PBDBT-2F:IT-4F	PBDBT-2F	-5.54	-3.65	IT-4F	-5.66	-4.14	0.710	19.00	67.00	9.72	0	201	3	1.40	0.12	0.49
PEDOT:PSS-DA	PNDIT-F3N	-5.14	-4.04	PM6:Y6	PM6	-5.50	-3.56	Y6	-5.65	-4.10	0.845	25.66	72.10	15.62	1	202	4	1.40	0.15	0.54
PEDOT:PSS	PNDIT-F3N	-5.00	-4.04	PM6:Y6	PM6	-5.50	-3.56	Y6	-5.65	-4.10	0.840	24.86	71.50	14.91	1	202	4	1.40	0.15	0.54
MoO3	TiO2/CT21	-6.30	-3.83	P3HT:PCBM	P3HT	-5.20	-3.30	PCBM	-6.10	-3.70	0.610	6.68	66.70	2.72	0	201	5	1.50	0.90	0.40
MoO3	TiO2/CT23	-6.30	-3.81	P3HT:PCBM	P3HT	-5.20	-3.30	PCBM	-6.10	-3.70	0.610	6.93	69.00	2.91	0	201	5	1.50	0.90	0.40
MoO3	TiO2	-6.30	-4.32	P3HT:PCBM	P3HT	-5.20	-3.30	PCBM	-6.10	-3.70	0.600	6.63	66.60	2.65	0	201	5	1.50	0.90	0.40
PEDOT:PSS	PDINN	-5.10	-3.72	PM6:Y6	PM6	-5.50	-3.56	Y6	-5.65	-4.10	0.847	25.89	78.59	17.23	1	202	6	1.40	0.15	0.54
PEDOT:PSS	PDINO	-5.10	-3.88	PM6:Y6	PM6	-5.50	-3.56	Y6	-5.65	-4.10	0.821	25.58	72.24	15.17	1	202	6	1.40	0.15	0.54
PEDOT:PSS	LiF	-5.20	-4.16	P3HT:PCBM	P3HT	-4.80	-2.95	PCBM	-6.20	-3.80	0.590	9.83	68.00	3.95	0	201	7	1.00	1.40	0.85
PCP-H	PFN-Br	-5.11	-2.80	J52-2F:IT-M	J52-2F	-5.16	-4.50	IT-M	-5.58	-3.98	0.960	18.40	73.00	12.80	1	201	8	1.18	0.42	0.52
PCP-Li	PFN-Br	-5.03	-2.80	J52-2F:IT-M	J52-2F	-5.16	-4.50	IT-M	-5.58	-3.98	0.930	18.30	69.80	11.80	1	201	8	1.18	0.42	0.52
PCP-Na	PFN-Br	-4.98	-2.80	J52-2F:IT-M	J52-2F	-5.16	-4.50	IT-M	-5.58	-3.98	0.910	18.00	67.20	11.00	1	201	8	1.18	0.42	0.52
PCP-K	PFN-Br	-4.87	-2.80	J52-2F:IT-M	J52-2F	-5.16	-4.50	IT-M	-5.58	-3.98	0.870	17.50	65.40	9.99	1	201	8	1.18	0.42	0.52
PCP-Cs	PFN-Br	-4.78	-2.80	J52-2F:IT-M	J52-2F	-5.16	-4.50	IT-M	-5.58	-3.98	0.840	17.10	64.60	9.10	1	201	8	1.18	0.42	0.52
MoO3	ZnO	-5.49	-4.17	PBDTTT-C-	PBDTTT-C-	-5.11	-3.25	PC70BM	-5.87	-3.91	0.750	14.89	59.00	6.58	0	201	9	1.20	0.76	0.66
MoO3	SASB	-5.49	-4.22	PBDTTT-C-	PBDTTT-C-	-5.11	-3.25	PC70BM	-5.87	-3.91	0.750	13.66	61.00	6.21	0	201	9	1.20	0.76	0.66
PEDOT:PSS	PAMPS-Na	-5.00	-3.24	PBDT-ST1:PC71BM	PBDT-ST1	-5.53	-3.57	PC71BM	-6.10	-3.90	0.890	13.62	73.00	9.09	1	201	10	1.25	0.95	0.59
PEDOT:PSS	PAMPS-Na	-5.00	-3.24	PTB7-Th:PC71BM	PTB7-Th	-5.24	-3.62	PC71BM	-6.10	-3.90	0.800	15.76	70.00	9.16	1	201	10	1.34	0.86	0.28
PEDOT:PSS	PAMPS-Na	-5.00	-3.24	PTB7:PC71BM	PTB7	-5.15	-3.31	PC71BM	-6.10	-3.90	0.790	15.64	64.00	8.24	0	201	10	1.63	0.57	0.33
MXene/PEDOT:PSS	PDINO	-5.22	-3.50	PBDB-T:ITIC	PBDB-T	-5.33	-2.92	ITIC	-5.51	-3.50	0.860	13.98	64.00	7.70	1	201	11	1.22	0.58	0.36
MXene/PEDOT:PSS	PrC60MA	-5.22	-3.90	PTB7-Th:PC71BM	PTB7-Th	-5.22	-3.64	PC71BM	-5.80	-4.00	0.790	14.62	61.00	7.16	0	201	11	1.83	0.18	0.58
PEDOT:PSS	PAMAM	-5.05	-4.06	PBDB-T:ITIC	PBDB-T	-5.33	-2.92	ITIC	-5.51	-3.78	0.890	16.77	62.00	9.25	1	201	12	1.55	0.18	0.86
PEDOT:PSS/4083	PDINO	-5.05	-3.63	PBDB-T:IT-M	PBDB-T	-5.21	-3.41	IT-M	-5.48	-3.83	0.930	14.75	68.71	9.42	1	201	13	1.38	0.27	0.42
PEDOT:PSS/Room-T	PDINO	-4.91	-3.63	PBDB-T:IT-M	PBDB-T	-5.21	-3.41	IT-M	-5.48	-3.83	0.925	16.01	71.61	10.60	1	201	13	1.38	0.27	0.42
PEDOT:PSS/High-T	PDINO	-4.80	-3.63	PBDB-T:IT-M	PBDB-T	-5.21	-3.41	IT-M	-5.48	-3.83	0.890	15.90	67.98	9.58	1	201	13	1.38	0.27	0.42
PEDOT:PSS	Bis-C60	-5.00	-3.90	PCE10:PC71BM	PCE10	-5.20	-3.60	PC71BM	-6.00	-3.90	0.790	16.38	66.10	8.60	0	201	14	1.30	0.80	0.30
PhNa-1T	Bis-C60	-5.20	-3.90	PCE10:PC71BM	PCE10	-5.20	-3.60	PC71BM	-6.00	-3.90	0.790	17.07	71.10	9.66	0	201	14	1.30	0.80	0.30

PEDOT:PSS	TiO2	-5.00	-4.30	PCE10:PC71BM	PCE10	-5.20	-3.60	PC71BM	-6.00	-3.90	0.790	16.18	63.70	8.11	0	201	14	1.30	0.80	0.30
PhNa-1T	TiO2	-5.20	-4.30	PCE10:PC71BM	PCE10	-5.20	-3.60	PC71BM	-6.00	-3.90	0.790	16.75	67.00	8.85	0	201	14	1.30	0.80	0.30
PEDOT:PSS	TiO2	-5.00	-4.30	PTB7:PC71BM	PTB7	-5.20	-3.60	PC71BM	-6.00	-3.90	0.750	15.19	66.00	7.51	0	201	14	1.30	0.80	0.30
PhNa-1P	TiO2	-5.40	-4.30	PTB7:PC71BM	PTB7	-5.20	-3.60	PC71BM	-6.00	-3.90	0.750	14.73	32.00	3.52	0	201	14	1.30	0.80	0.30
PhNa-1T	TiO2	-5.20	-4.30	PTB7:PC71BM	PTB7	-5.20	-3.60	PC71BM	-6.00	-3.90	0.750	16.05	68.60	8.26	0	201	14	1.30	0.80	0.30
PhNa-2T	TiO2	-5.20	-4.30	PTB7:PC71BM	PTB7	-5.20	-3.60	PC71BM	-6.00	-3.90	0.750	15.62	67.10	7.93	0	201	14	1.30	0.80	0.30
PhNa-3T	TiO2	-5.10	-4.30	PTB7:PC71BM	PTB7	-5.20	-3.60	PC71BM	-6.00	-3.90	0.740	16.17	62.90	7.54	0	201	14	1.30	0.80	0.30
MoO3	ZnO/S-GQD	-5.60	-3.95	PTB7:PC71BM	PTB7	-5.15	-3.31	PC71BM	-6.00	-4.00	0.760	17.24	73.00	9.56	0	201	15	1.15	0.85	0.69
MoO3	ZnO/M-GQD	-5.60	-4.07	PTB7:PC71BM	PTB7	-5.15	-3.31	PC71BM	-6.00	-4.00	0.760	17.91	74.50	10.14	0	201	15	1.15	0.85	0.69
MoO3	ZnO/L-GQD	-5.60	-4.26	PTB7:PC71BM	PTB7	-5.15	-3.31	PC71BM	-6.00	-4.00	0.760	17.47	73.60	9.77	0	201	15	1.15	0.85	0.69
MoO3	ZnO	-5.60	-4.40	PTB7:PC71BM	PTB7	-5.15	-3.31	PC71BM	-6.00	-4.00	0.750	16.80	69.50	8.76	0	201	15	1.15	0.85	0.69
PEDOT:PSS	CTOC-N-Br	-5.10	-4.09	PM6:BTP-4Cl	PM6	-5.00	-2.62	BTP-4Cl	-5.66	-4.09	0.840	26.57	77.00	17.19	1	202	16	0.91	0.66	1.47
PEDOT:PSS	CTOC-N	-5.10	-4.37	PM6:BTP-4Cl	PM6	-5.00	-2.62	BTP-4Cl	-5.66	-4.09	0.822	26.28	75.00	16.22	1	202	16	0.91	0.66	1.47
PEDOT:PSS	CTOC	-5.10	-4.19	PM6:BTP-4Cl	PM6	-5.00	-2.62	BTP-4Cl	-5.66	-4.09	0.810	26.02	71.00	15.05	1	202	16	0.91	0.66	1.47
GO:F5BnPA	Ca	-5.52	-2.70	SMPV1:PC71BM	SMPV1	-5.50	-3.50	PC71BM	-5.80	-4.00	0.920	11.96	46.59	5.13	1	201	17	1.50	0.30	0.50
MoOx:F5BnPA	Ca	-5.58	-2.70	SMPV1:PC71BM	SMPV1	-5.50	-3.50	PC71BM	-5.80	-4.00	0.910	11.69	55.92	5.96	1	201	17	1.50	0.30	0.50
MoOx	Ca	-5.35	-2.70	SMPV1:PC71BM	SMPV1	-5.50	-3.50	PC71BM	-5.80	-4.00	0.880	10.96	50.81	4.92	1	201	17	1.50	0.30	0.50
GO	Ca	-4.92	-2.70	SMPV1:PC71BM	SMPV1	-5.50	-3.50	PC71BM	-5.80	-4.00	0.650	11.03	43.28	3.10	0	201	17	1.50	0.30	0.50
MoOx	Ba(OH)2	-5.49	-3.80	PTB7-Th:PC70BM	PTB7-Th	-5.22	-3.64	PC70BM	-6.10	-4.30	0.818	15.69	67.60	8.66	1	201	18	0.92	0.88	0.66
MoOx	ZnO	-5.49	-4.30	PTB7-Th:PC70BM	PTB7-Th	-5.22	-3.64	PC70BM	-6.10	-4.30	0.803	14.28	62.30	7.12	1	201	18	0.92	0.88	0.66
PEDOT:PSS	PDINO	-5.11	-3.64	PTQ10:IDIC	PTQ10	-5.54	-2.98	IDIC	-5.73	-3.91	0.960	16.80	72.02	11.56	1	201	19	1.61	0.26	0.95
PEDOT:PSS-GO	PDINO-G	-5.00	-3.86	PTQ10:IDIC	PTQ10	-5.54	-2.98	IDIC	-5.73	-3.91	0.960	17.43	74.34	12.44	1	201	19	1.61	0.26	0.95
PEDOT:PSS-GO	PDINO-G	-5.00	-3.86	PTQ10:IDIC-2F	PTQ10	-5.54	-2.98	IDIC-2F	-5.80	-3.93	0.910	19.09	74.87	13.01	1	201	19	1.61	0.26	0.95
PEDOT:PSS	PDINO-G	-5.11	-3.86	PTQ10:IDIC-2F	PTQ10	-5.54	-2.98	IDIC-2F	-5.80	-3.93	0.910	18.57	74.43	12.58	1	201	19	1.61	0.26	0.95
PEDOT:PSS	PDINO	-5.11	-3.64	PTQ10:IDIC-2F	PTQ10	-5.54	-2.98	IDIC-2F	-5.80	-3.93	0.900	18.06	72.66	11.81	1	201	19	1.46	0.09	0.60
PEDOT:PSS-GO	PDINO	-5.00	-3.64	PTQ10:IDIC-2F	PTQ10	-5.54	-2.98	IDIC-2F	-5.80	-3.93	0.900	18.39	73.92	12.23	1	201	19	1.46	0.09	0.60
PEDOT:PSS-GO	PDINO-G	-5.00	-3.86	PM6:Y6	PM6	-5.56	-3.50	Y6	-5.65	-4.10	0.850	25.65	75.78	16.52	1	201	19	1.63	0.19	0.93
PEDOT:PSS	PDINO	-5.11	-3.64	PM6:Y6	PM6	-5.56	-3.50	Y6	-5.65	-4.10	0.840	24.84	73.43	15.32	1	201	19	1.63	0.19	0.93
MoO3	SnO2	-5.60	-4.06	PM6:IT-4F	PM6	-5.56	-3.50	IT-4F	-5.59	-3.50	0.850	21.30	78.00	14.10	1	201	20	2.06	0.03	0.00
MoO3	ZnO	-5.60	-3.80	PM6:IT-4F	PM6	-5.56	-3.50	IT-4F	-5.59	-3.50	0.840	20.70	75.00	13.00	1	201	20	2.06	0.03	0.00
U-MXene	Ca	-5.01	-2.70	PBDB-T:ITIC	PBDB-T	-5.33	-2.92	ITIC	-5.51	-3.78	0.890	15.98	64.00	9.02	1	201	21	1.55	0.18	0.86
MoO3	UH-MXene	-5.49	-4.30	PBDB-T:ITIC	PBDB-T	-5.33	-2.92	ITIC	-5.51	-3.78	0.870	17.36	60.00	9.06	1	201	21	1.55	0.18	0.86
MoOx	ZnO/PEIE	-5.60	-4.00	M1:PC70BM	M1	-5.29	-3.45	PC70BM	-5.87	-3.91	0.897	12.50	61.60	6.91	1	201	22	1.38	0.58	0.46
MoOx	ZnO	-5.60	-4.50	M1:PC70BM	M1	-5.29	-3.45	PC70BM	-5.87	-3.91	0.855	11.90	61.50	6.25	1	201	22	1.38	0.58	0.46
0.1MHClO4-	PDINN	-5.39	-3.72	PM6:Y6	PM6	-5.56	-3.50	Y6	-5.65	-4.10	0.850	25.83	74.80	16.44	1	202	23	1.46	0.09	0.60
0.1MHClO4-	PDINO	-5.39	-3.88	PM6:Y6	PM6	-5.56	-3.50	Y6	-5.65	-4.10	0.850	24.49	73.20	15.24	1	202	23	1.46	0.09	0.60
CH3SO3H-	PDINN	-4.91	-3.72	PM6:Y6	PM6	-5.56	-3.50	Y6	-5.65	-4.10	0.830	24.71	68.30	14.01	1	202	23	1.46	0.09	0.60
PEDOT:PSS	PFN/NBR	-5.00	-4.92	PTB7-Th:PC71BM	PTB7-Th	-5.31	-3.72	PC71BM	-6.10	-3.90	0.800	15.27	53.00	6.49	1	201	24	1.41	0.79	0.18

MoO3	PFN/NBR	-5.60	-4.92	PTB7-Th:PC71BM	PTB7-Th	-5.31	-3.72	PC71BM	-6.10	-3.90	0.730	15.95	56.00	6.59	0	201	24	1.41	0.79	0.18
MoO3	PFN	-5.60	-5.02	PTB7-Th:PC71BM	PTB7-Th	-5.31	-3.72	PC71BM	-6.10	-3.90	0.610	13.56	54.00	4.41	0	201	24	1.41	0.79	0.18
MoO3	NBR	-5.60	-4.97	PTB7-Th:PC71BM	PTB7-Th	-5.31	-3.72	PC71BM	-6.10	-3.90	0.550	14.68	54.00	4.29	0	201	24	1.41	0.79	0.18
MoO3	ZnO/L-Arg	-5.30	-3.74	PTB7-Th:PC71BM	PTB7-Th	-5.20	-3.64	PC71BM	-6.10	-4.00	0.780	17.49	68.22	9.31	0	201	25	1.20	0.90	0.36
MoO3	ZnO	-5.30	-4.34	PTB7-Th:PC71BM	PTB7-Th	-5.20	-3.64	PC71BM	-6.10	-4.00	0.770	16.30	64.45	8.09	0	201	25	1.20	0.90	0.36
MoO3	L-Arg	-5.30	-3.97	PTB7-Th:PC71BM	PTB7-Th	-5.20	-3.64	PC71BM	-6.10	-4.00	0.770	17.25	67.80	9.00	0	201	25	1.20	0.90	0.36
PH1000/Gra	Ca	-4.90	-2.90	PCDTBT:PC71BM	PCDTBT	-5.50	-3.60	PC71BM	-6.00	-4.00	0.840	12.63	42.35	4.44	1	201	26	1.50	0.50	0.40
PH1000	Ca	-5.00	-2.90	PCDTBT:PC71BM	PCDTBT	-5.50	-3.60	PC71BM	-6.00	-4.00	0.820	9.03	41.78	3.09	1	201	26	1.50	0.50	0.40
Gra	Ca	-4.60	-2.90	PCDTBT:PC71BM	PCDTBT	-5.50	-3.60	PC71BM	-6.00	-4.00	0.800	9.45	35.56	2.68	1	201	26	1.50	0.50	0.40
MoOx	LiF	-6.00	-2.60	PTB7:PCBM	PTB7	-5.20	-3.30	PCBM	-6.10	-4.00	0.740	15.50	64.00	7.31	0	201	27	1.20	0.90	0.50
PEDOT:PSS/CNT	LiF	-5.40	-2.60	PTB7:PCBM	PTB7	-5.20	-3.30	PCBM	-6.10	-4.00	0.720	13.70	61.00	6.04	0	201	27	1.20	0.90	0.70
MoOx	LiF	-6.00	-2.60	P3HT:PCBM	P3HT	-5.20	-3.50	PCBM	-6.10	-4.00	0.600	9.42	50.00	2.83	0	201	27	1.20	0.90	0.50
PEDOT:PSS/CNT	LiF	-5.40	-2.60	P3HT:PCBM	P3HT	-5.20	-3.50	PCBM	-6.10	-4.00	0.590	8.84	46.00	2.43	0	201	27	1.20	0.90	0.70
HPMO:Sn	PFN-Br	-5.42	-2.70	PBDB-T:ITIC	PBDB-T	-5.33	-2.92	ITIC	-5.51	-3.78	0.900	16.62	70.80	10.59	1	202	28	1.42	0.17	0.49
HPMO:Sn	PFN-Br	-5.42	-2.70	PM6:IT-4F	PM6	-5.48	-3.66	IT-4F	-5.65	-4.12	0.860	20.25	76.40	13.34	1	202	28	1.22	0.58	0.36
HPMO:Sn	PFN-Br	-5.42	-2.70	PM6:BTP-eC9	PM6(PBDB-	-5.47	-3.56	BTP-eC9	-5.64	-4.05	0.840	26.80	77.00	17.30	1	202	28	1.55	0.18	0.86
HPMO:Sn	PFN-Br	-5.42	-2.70	PTB7-Th:PC71BM	PTB7-Th	-5.22	-3.64	PC71BM	-5.80	-4.00	0.800	16.59	64.60	8.57	1	202	28	1.36	0.17	0.46
IZO-MoO3	Ca	-5.23	-2.98	P3HT:PCBM	P3HT	-5.00	-3.00	PCBM	-6.50	-4.00	0.601	7.87	64.06	3.03	0	201	29	1.00	1.50	1.00
MIZO	Ca	-5.17	-2.98	P3HT:PCBM	P3HT	-5.00	-3.00	PCBM	-6.50	-4.00	0.592	8.12	66.53	3.20	0	201	29	1.00	1.50	1.00
IZO	Ca	-5.05	-2.98	P3HT:PCBM	P3HT	-5.00	-3.00	PCBM	-6.50	-4.00	0.535	8.00	64.94	2.79	0	201	29	1.00	1.50	1.00
PEDOT:PSS	PFN	-5.10	-4.30	PTB7-Th:PC71BM	PTB7-Th	-5.20	-3.60	PC71BM	-6.00	-4.30	0.780	15.60	72.00	8.76	0	201	30	0.90	0.80	0.70
p-PFP-MD	PFN	-5.05	-4.30	PTB7-Th:PC71BM	PTB7-Th	-5.20	-3.60	PC71BM	-6.00	-4.30	0.780	15.90	70.00	8.70	0	201	30	0.90	0.80	0.70
p-PFP-HD	PFN	-5.14	-4.30	PTB7-Th:PC71BM	PTB7-Th	-5.20	-3.60	PC71BM	-6.00	-4.30	0.780	16.30	71.00	9.03	0	201	30	0.90	0.80	0.70
p-PFP-WD	PFN	-4.99	-4.30	PTB7-Th:PC71BM	PTB7-Th	-5.20	-3.60	PC71BM	-6.00	-4.30	0.750	15.60	61.00	7.19	0	201	30	0.90	0.80	0.70
MoO3	ZnO-C60	-5.49	-4.53	PTB7-Th:PC71BM	PTB7-Th	-5.22	-3.64	PC71BM	-5.80	-4.00	0.800	15.73	74.30	9.35	1	201	31	1.14	0.66	0.49
MoO3	ZnO	-5.49	-4.14	PTB7-Th:PC71BM	PTB7-Th	-5.22	-3.64	PC71BM	-5.80	-4.00	0.790	14.02	69.10	7.64	0	201	31	1.14	0.66	0.49
MoO3	ZnO-C60	-5.49	-4.53	PTB7:PC71BM	PTB7	-5.14	-3.51	PC71BM	-5.80	-4.00	0.730	15.41	73.00	8.21	0	201	31	1.22	0.58	0.36
MoO3	ZnO	-5.49	-4.14	PTB7:PC71BM	PTB7	-5.14	-3.51	PC71BM	-5.80	-4.00	0.700	13.75	69.00	6.65	0	201	31	1.22	0.58	0.36
PEDOT:PSS	PFN-Br	-4.80	-3.00	PBDB-T-SF:IT-4F	PBDB-T-SF	-5.42	-3.64	IT-4F	-5.70	-4.10	0.900	20.20	72.00	13.10	1	201	32	1.32	0.28	0.46
WS2	PFN-Br	-5.50	-3.00	PBDB-T-SF:IT-4F	PBDB-T-SF	-5.42	-3.64	IT-4F	-5.70	-4.10	0.880	20.60	74.00	13.50	1	201	32	1.32	0.28	0.46
PEDOT:PSS	PFN-Br	-4.80	-3.00	PBDB-T-SF:Y6	PBDB-T-SF	-5.42	-3.64	Y6	-5.60	-4.30	0.850	25.20	72.00	15.30	1	201	32	1.32	0.28	0.46
MoS2	PFN-Br	-5.40	-3.00	PBDB-T-SF:IT-4F	PBDB-T-SF	-5.42	-3.64	IT-4F	-5.70	-4.10	0.840	20.00	71.00	12.00	1	201	32	1.12	0.18	0.66
WS2	PFN-Br	-5.50	-3.00	PBDB-T-SF:Y6	PBDB-T-SF	-5.42	-3.64	Y6	-5.60	-4.30	0.840	25.90	73.00	15.80	1	201	32	1.12	0.18	0.66
PEDOT:PSS	PFN-Br	-5.15	-2.85	PM6:BTP-eC9	PM6	-5.25	-2.91	BTP-eC9	-5.87	-3.89	0.854	26.28	78.20	17.52	1	202	33	1.39	0.61	0.95
2PACz	PFN-Br	-5.45	-2.85	PM6:BTP-eC9	PM6	-5.25	-2.91	BTP-eC9	-5.87	-3.89	0.845	26.94	79.20	18.03	1	202	33	1.39	0.61	0.95
PEDOT:PSS	PFN-Br	-5.15	-2.85	PM6:N3	PM6	-5.25	-2.91	N3	-5.86	-3.86	0.842	25.64	73.90	15.94	1	202	33	1.36	0.62	0.98
2PACz	PFN-Br	-5.45	-2.85	PM6:N3	PM6	-5.25	-2.91	N3	-5.86	-3.86	0.840	26.53	74.50	16.60	1	202	33	1.36	0.62	0.98
PEDOT:PSS-PA	PNDIT-F3N	-5.49	-3.95	PM6:ITC-2Cl	PM6	-5.50	-3.61	ITC-2Cl	-5.58	-4.01	0.919	19.56	75.70	13.62	1	202	34	1.40	0.10	0.49

PEDOT:PSS-TA	PNDIT-F3N	-5.47	-3.95	PM6:ITC-2Cl	PM6	-5.50	-3.61	ITC-2Cl	-5.58	-4.01	0.917	19.60	77.10	13.87	1	202	34	1.40	0.10	0.49
PEDOT:PSS-DA	PNDIT-F3N	-5.38	-3.95	PM6:ITC-2Cl	PM6	-5.50	-3.61	ITC-2Cl	-5.58	-4.01	0.916	20.06	77.10	14.17	1	202	34	1.40	0.10	0.49
PEDOT:PSS	PNDIT-F3N	-5.34	-3.95	PM6:ITC-2Cl	PM6	-5.50	-3.61	ITC-2Cl	-5.58	-4.01	0.912	19.48	75.50	13.42	1	202	34	1.40	0.10	0.49
PEDOT:PSS-PA	PNDIT-F3N	-5.49	-3.95	PM6:Y6	PM6	-5.50	-3.61	Y6	-5.60	-4.10	0.853	25.50	77.60	16.88	1	202	34	1.49	0.08	0.40
PEDOT:PSS-TA	PNDIT-F3N	-5.47	-3.95	PM6:Y6	PM6	-5.50	-3.61	Y6	-5.60	-4.10	0.846	25.82	78.20	17.10	1	202	34	1.49	0.08	0.40
PEDOT:PSS-DA	PNDIT-F3N	-5.38	-3.95	PM6:Y6	PM6	-5.50	-3.61	Y6	-5.60	-4.10	0.845	25.64	77.70	16.83	1	202	34	1.49	0.08	0.40
PEDOT:PSS	PNDIT-F3N	-5.34	-3.95	PM6:Y6	PM6	-5.50	-3.61	Y6	-5.60	-4.10	0.840	25.47	77.10	16.52	1	202	34	1.49	0.08	0.40
PEDOT:PSS-PA	PNDIT-F3N	-5.49	-3.95	PM6:PIDTC-T	PM6	-5.50	-3.61	PIDTC-T	-5.99	-4.05	0.831	16.34	70.40	9.55	1	202	34	1.45	0.49	0.44
PEDOT:PSS-TA	PNDIT-F3N	-5.47	-3.95	PM6:PIDTC-T	PM6	-5.50	-3.61	PIDTC-T	-5.99	-4.05	0.830	16.16	67.60	9.07	1	202	34	1.45	0.49	0.44
PEDOT:PSS-DA	PNDIT-F3N	-5.38	-3.95	PM6:PIDTC-T	PM6	-5.50	-3.61	PIDTC-T	-5.99	-4.05	0.825	15.81	64.30	8.38	1	202	34	1.45	0.49	0.44
PEDOT:PSS	PNDIT-F3N	-5.34	-3.95	PM6:PIDTC-T	PM6	-5.50	-3.61	PIDTC-T	-5.99	-4.05	0.821	15.27	56.20	7.05	1	202	34	1.45	0.49	0.44
PEDOT:PSS	PFN-2TNDI	-5.10	-4.00	PBDB-T:ITIC	PBDB-T	-5.33	-2.92	ITIC	-5.48	-3.83	0.920	16.59	70.00	11.10	1	201	35	1.50	0.15	0.91
PEDOT:PSS	PFN	-5.10	-4.20	PBDB-T:ITIC	PBDB-T	-5.33	-2.92	ITIC	-5.48	-3.83	0.910	15.80	58.00	8.60	1	201	35	1.50	0.15	0.91
PEDOT:PSS	PFN-2TNDI	-5.10	-4.00	PTB7-Th:N2200	PTB7-Th	-5.20	-3.59	N2200	-5.77	-3.84	0.780	13.69	58.00	6.30	0	201	35	1.36	0.57	0.25
PEDOT:PSS	Ca	-5.10	-2.90	PTB7-Th:N2200	PTB7-Th	-5.20	-3.59	N2200	-5.77	-3.84	0.780	12.69	55.00	5.60	0	201	35	1.36	0.57	0.25
PEDOT:PSS	PFN	-5.10	-4.20	PTB7-Th:N2200	PTB7-Th	-5.20	-3.59	N2200	-5.77	-3.84	0.770	13.18	51.00	5.40	0	201	35	1.36	0.57	0.25
PEDOT:PSS	MSAPBS	-5.10	-3.01	PTB7-Th:PC71BM	PTB7-Th	-5.40	-3.80	PC71BM	-6.10	-4.10	0.790	18.15	59.80	8.56	0	201	36	0.90	1.10	1.10
O-MoS2-QDs	MSAPBS	-5.20	-3.01	PTB7-Th:PC71BM	PTB7-Th	-5.40	-3.80	PC71BM	-6.10	-4.10	0.790	16.90	65.00	8.66	0	201	36	0.90	1.10	1.10
O-MoS2-QDs	Ca	-5.20	-2.90	PTB7-Th:PC71BM	PTB7-Th	-5.40	-3.80	PC71BM	-6.10	-4.10	0.780	16.74	59.20	7.71	0	201	36	0.90	1.10	1.10
PEDOT:PSS	Ca	-5.10	-2.90	PTB7-Th:PC71BM	PTB7-Th	-5.40	-3.80	PC71BM	-6.10	-4.10	0.740	16.53	62.50	7.63	0	201	36	1.30	0.70	0.30
MoS2-QDs	MSAPBS	-4.40	-3.01	PTB7-Th:PC71BM	PTB7-Th	-5.40	-3.80	PC71BM	-6.10	-4.10	0.630	14.01	57.00	5.09	0	201	36	1.30	0.70	0.30
O-MoS2-QDs	Ca	-5.20	-2.90	P3HT:PC61BM	P3HT	-5.00	-3.00	PC61BM	-6.10	-4.10	0.570	7.28	63.40	2.62	0	201	36	1.30	0.70	0.30
PEDOT:PSS	Ca	-5.10	-2.90	P3HT:PC61BM	P3HT	-5.00	-3.00	PC61BM	-6.10	-4.10	0.560	8.21	59.10	2.70	0	201	36	1.30	0.70	0.30
MoS2-QDs	Ca	-4.40	-2.90	PTB7-Th:PC71BM	PTB7-Th	-5.40	-3.80	PC71BM	-6.10	-4.10	0.550	14.58	53.10	4.23	0	201	36	1.30	0.70	0.30
MoS2-QDs	Ca	-4.40	-2.90	P3HT:PC61BM	P3HT	-5.00	-3.00	PC61BM	-6.10	-4.10	0.320	6.08	42.30	0.81	0	201	36	1.30	0.70	0.30
MoO3	eLbL	-5.50	-4.30	PTB7-Th:PC71BM	PTB7-Th	-5.40	-3.80	PC71BM	-6.00	-4.20	0.760	20.00	67.00	10.18	0	201	37	1.20	0.60	0.40
PEDOT:PSS	LiF	-5.10	-4.10	PCDTBT:PC71BM	PCDTBT	-5.50	-3.60	PC71BM	-6.10	-4.30	0.900	10.11	66.00	6.02	1	201	38	0.85	0.95	0.99
F-GQD	LiF	-5.26	-4.10	PCDTBT:PC71BM	PCDTBT	-5.50	-3.60	PC71BM	-6.10	-4.30	0.890	10.65	67.00	6.30	1	201	38	0.85	0.95	0.99
F-GQD	LiF	-5.26	-4.10	PTB7:PC71BM	PTB7	-5.15	-3.31	PC71BM	-6.10	-4.30	0.750	15.20	69.00	7.91	0	201	38	0.85	0.95	0.99
PEDOT:PSS	LiF	-5.10	-4.10	PTB7:PC71BM	PTB7	-5.15	-3.31	PC71BM	-6.10	-4.30	0.740	13.96	72.00	7.46	0	201	38	1.20	0.60	0.70
GO	LiF	-5.01	-4.10	PTB7:PC71BM	PTB7	-5.15	-3.31	PC71BM	-6.10	-4.30	0.690	13.58	68.00	6.33	0	201	38	1.20	0.60	0.70
GO	LiF	-5.01	-4.10	PCDTBT:PC71BM	PCDTBT	-5.50	-3.60	PC71BM	-6.10	-4.30	0.670	9.97	65.00	4.34	0	201	38	1.20	0.60	0.70
PEDOT:PSS	TiOx	-5.10	-4.30	PCDTBT:PC71BM	PCDTBT	-5.50	-3.60	PC71BM	-6.00	-4.30	0.880	11.28	55.60	5.61	1	201	39	1.20	0.50	0.70
GO	TiOx	-4.95	-4.30	PCDTBT:PC71BM	PCDTBT	-5.50	-3.60	PC71BM	-6.00	-4.30	0.880	11.52	55.10	5.71	1	201	39	1.20	0.50	0.70
GO-Cl1	TiOx	-5.04	-4.30	PCDTBT:PC71BM	PCDTBT	-5.50	-3.60	PC71BM	-6.00	-4.30	0.880	11.78	55.10	5.82	1	201	39	1.20	0.50	0.70
GO-Cl2	TiOx	-5.11	-4.30	PCDTBT:PC71BM	PCDTBT	-5.50	-3.60	PC71BM	-6.00	-4.30	0.880	12.19	55.20	6.07	1	201	39	1.20	0.50	0.70
GO-Cl3	TiOx	-5.16	-4.30	PCDTBT:PC71BM	PCDTBT	-5.50	-3.60	PC71BM	-6.00	-4.30	0.880	13.32	55.10	6.61	1	201	39	1.20	0.50	0.70
GO-Cl4	TiOx	-5.23	-4.30	PCDTBT:PC71BM	PCDTBT	-5.50	-3.60	PC71BM	-6.00	-4.30	0.880	13.65	55.30	6.79	1	201	39	1.20	0.50	0.70

PEDOT:PSS	TiOx	-5.10	-4.30	PTB7:PC71BM	PTB7	-5.15	-3.30	PC71BM	-6.00	-4.30	0.760	16.27	59.80	7.60	0	201	39	0.85	0.85	1.00
GO	TiOx	-4.95	-4.30	PTB7:PC71BM	PTB7	-5.15	-3.30	PC71BM	-6.00	-4.30	0.760	16.65	59.70	7.74	0	201	39	0.85	0.85	1.00
GO-Cl1	TiOx	-5.04	-4.30	PTB7:PC71BM	PTB7	-5.15	-3.30	PC71BM	-6.00	-4.30	0.760	17.13	59.60	7.93	0	201	39	0.85	0.85	1.00
GO-Cl2	TiOx	-5.11	-4.30	PTB7:PC71BM	PTB7	-5.15	-3.30	PC71BM	-6.00	-4.30	0.760	17.58	59.60	8.19	0	201	39	0.85	0.85	1.00
GO-Cl3	TiOx	-5.16	-4.30	PTB7:PC71BM	PTB7	-5.15	-3.30	PC71BM	-6.00	-4.30	0.760	18.30	59.90	8.52	0	201	39	0.85	0.85	1.00
GO-Cl4	TiOx	-5.23	-4.30	PTB7:PC71BM	PTB7	-5.15	-3.30	PC71BM	-6.00	-4.30	0.760	17.09	59.50	7.91	0	201	39	0.85	0.85	1.00
MoO3	ZnO/C-dots	-5.30	-3.50	PTB7:PC71BM	PTB7	-5.20	-3.30	PC71BM	-6.10	-4.20	0.750	17.59	68.27	9.08	0	201	40	1.00	0.90	0.90
MoO3	AZ0/C-dots	-5.30	-3.39	PTB7:PC71BM	PTB7	-5.20	-3.30	PC71BM	-6.10	-4.20	0.750	17.65	69.50	9.28	0	201	40	1.00	0.90	0.90
MoO3	ZnO	-5.30	-3.89	PTB7:PC71BM	PTB7	-5.20	-3.30	PC71BM	-6.10	-4.20	0.730	15.23	67.11	7.54	0	201	40	1.00	0.90	0.90
MoO3	AZ0	-5.30	-3.80	PTB7:PC71BM	PTB7	-5.20	-3.30	PC71BM	-6.10	-4.20	0.730	16.19	67.43	8.06	0	201	40	1.00	0.90	0.90
MoO3	PFN100	-5.30	-3.60	P3HT:PC61BM	P3HT	-5.00	-3.00	PC61BM	-6.00	-4.20	0.630	7.86	66.00	3.27	0	201	41	0.80	1.00	1.20
MoO3	PFN70	-5.30	-3.69	P3HT:PC61BM	P3HT	-5.00	-3.00	PC61BM	-6.00	-4.20	0.620	7.84	62.00	3.01	0	201	41	0.80	1.00	1.20
MoO3	PFN50	-5.30	-3.73	P3HT:PC61BM	P3HT	-5.00	-3.00	PC61BM	-6.00	-4.20	0.610	7.51	56.10	2.57	0	201	41	0.80	1.00	1.20
MoO3	PFN30	-5.30	-3.86	P3HT:PC61BM	P3HT	-5.00	-3.00	PC61BM	-6.00	-4.20	0.600	7.00	54.80	2.31	0	201	41	0.80	1.00	1.20
PEDOT:PSS	PFN-Br	-4.85	-2.80	PBDB-TF:PC71BM	PBDB-TF	-5.45	-3.65	PC71BM	-6.10	-4.20	0.980	13.37	73.20	9.59	1	201	42	1.11	0.79	1.20
NFD:PEDOT:PSS	PFN-Br	-5.01	-2.80	PBDB-TF:PC71BM	PBDB-TF	-5.45	-3.65	PC71BM	-6.10	-4.20	0.980	13.82	79.44	10.76	1	201	42	1.11	0.79	1.20
PEDOT:PSS	PFN-Br	-4.85	-2.80	PDCBT:PC71BM	PDCBT	-5.31	-3.00	PC71BM	-6.10	-4.20	0.830	12.20	71.20	7.21	1	201	42	1.11	0.79	1.20
PSSS:PEDOT:PSS	PFN-Br	-4.80	-2.80	PDCBT:PC71BM	PDCBT	-5.31	-3.00	PC71BM	-6.10	-4.20	0.830	12.44	77.21	7.97	1	201	42	1.25	0.65	0.55
NFD	PFN-Br	-4.41	-2.80	PBDB-TF:PC71BM	PBDB-TF	-5.45	-3.65	PC71BM	-6.10	-4.20	0.520	13.57	46.85	3.31	0	201	42	1.25	0.65	0.55
PSSS	PFN-Br	-4.32	-2.80	PDCBT:PC71BM	PDCBT	-5.31	-3.00	PC71BM	-6.10	-4.20	0.450	12.31	42.12	2.28	0	201	42	1.25	0.65	0.55
PEDOT:PSS	ZnO	-5.13	-4.20	P3HT:PCBM	P3HT	-5.20	-3.20	PCBM	-6.10	-3.90	0.610	8.50	59.00	2.99	0	201	43	1.30	0.90	0.70
PEDOT:PSS@DOH	ZnO	-5.24	-4.20	P3HT:PCBM	P3HT	-5.20	-3.20	PCBM	-6.10	-3.90	0.600	9.13	63.00	3.44	0	201	43	1.30	0.90	0.70
WOx:PEDOT:PSS	PFN-Br	-4.70	-2.80	PBDB-TF:IT-4F	PBDB-TF	-5.50	-3.61	IT-4F	-5.69	-4.07	0.870	20.73	80.78	14.57	1	201	44	1.43	0.19	0.46
PEDOT:PSS	PFN-Br	-4.85	-2.80	PBDB-TF:IT-4F	PBDB-TF	-5.50	-3.61	IT-4F	-5.69	-4.07	0.870	20.68	73.87	13.29	1	201	44	1.43	0.19	0.46
WOx	PFN-Br	-4.73	-2.80	PBDB-TF:IT-4F	PBDB-TF	-5.50	-3.61	IT-4F	-5.69	-4.07	0.780	16.78	66.70	8.73	0	201	44	1.43	0.19	0.46
MoO3	ECGQD-K	-5.50	-4.33	PCDTBT:PC71BM	PCDTBT	-5.40	-3.20	PC71BM	-6.10	-4.30	0.880	9.70	67.00	5.72	1	201	45	1.10	0.70	1.10
MoO3	ECGQD-Rb	-5.50	-4.16	PCDTBT:PC71BM	PCDTBT	-5.40	-3.20	PC71BM	-6.10	-4.30	0.880	9.77	68.00	5.85	1	201	45	1.10	0.70	1.10
MoO3	ECGQD-Cs	-5.50	-4.03	PCDTBT:PC71BM	PCDTBT	-5.40	-3.20	PC71BM	-6.10	-4.30	0.880	9.92	68.00	5.94	1	201	45	1.10	0.70	1.10
MoO3	ECGQD-Na	-5.50	-4.41	PCDTBT:PC71BM	PCDTBT	-5.40	-3.20	PC71BM	-6.10	-4.30	0.730	9.54	55.00	3.83	0	201	45	1.10	0.70	1.10
MoO3	ECGQD-Li	-5.50	-4.47	PCDTBT:PC71BM	PCDTBT	-5.40	-3.20	PC71BM	-6.10	-4.30	0.590	9.57	49.00	2.77	0	201	45	1.10	0.70	1.10
PEDOT:PSS	ZnO	-5.14	-4.30	PTB7-Th:PC71BM	PTB7-Th	-5.24	-3.60	PC71BM	-5.90	-3.90	0.854	26.50	73.50	16.60	1	202	46	1.34	0.66	0.30
an-MoOx2	ZnO	-5.14	-4.30	PTB7-Th:PC71BM	PTB7-Th	-5.24	-3.60	PC71BM	-5.90	-3.90	0.845	27.43	73.80	17.10	1	202	46	1.34	0.66	0.30
aq-MoOx	ZnO	-4.92	-4.30	PTB7-Th:PC71BM	PTB7-Th	-5.24	-3.60	PC71BM	-5.90	-3.90	0.843	27.53	73.10	17.00	1	202	46	1.34	0.66	0.30
an-MoOx1	ZnO	-4.74	-4.30	PTB7-Th:PC71BM	PTB7-Th	-5.24	-3.60	PC71BM	-5.90	-3.90	0.826	20.50	45.20	7.70	1	202	46	1.34	0.66	0.30
PEDOT:PSS	ZnO	-5.14	-4.30	PBDB-T-2F:Y6	PBDB-T-2F	-5.60	-3.50	Y6	-5.70	-4.10	0.791	15.67	67.30	8.30	0	202	46	1.50	0.10	0.60
an-MoOxw	ZnO	-5.14	-4.30	PBDB-T-2F:Y6	PBDB-T-2F	-5.60	-3.50	Y6	-5.70	-4.10	0.791	16.60	68.20	9.00	0	202	46	1.50	0.10	0.60
aq-MoOx	ZnO	-4.92	-4.30	PBDB-T-2F:Y6	PBDB-T-2F	-5.60	-3.50	Y6	-5.70	-4.10	0.790	16.69	67.10	8.90	0	202	46	1.50	0.10	0.60
an-MoOxo	ZnO	-4.74	-4.30	PBDB-T-2F:Y6	PBDB-T-2F	-5.60	-3.50	Y6	-5.70	-4.10	0.683	4.25	47.90	1.40	0	202	46	1.50	0.10	0.60

MoOx	ZnO	-5.40	-4.40	PBDB-T:ITIC	PBDB-T	-5.33	-2.92	ITIC	-5.51	-3.78	0.890	16.61	67.71	10.01	1	202	47	1.55	0.18	0.86
F6-TCNNQ	ZnO	-5.60	-4.40	PBDB-T:ITIC	PBDB-T	-5.33	-2.92	ITIC	-5.51	-3.78	0.870	17.01	67.34	9.97	1	202	47	1.55	0.18	0.86
PEDOT:PSS:TS	PFN-Br	-5.18	-2.62	PTB7-Th:IEICO-4F	PTB7-Th	-5.22	-3.59	IEICO-4F	-5.44	-4.19	0.720	21.09	58.00	8.84	0	202	48	1.03	0.22	0.60
F4-TCNQ:TS	PFN-Br	-5.06	-2.62	PTB7-Th:IEICO-4F	PTB7-Th	-5.22	-3.59	IEICO-4F	-5.44	-4.19	0.720	24.36	54.67	9.59	0	202	48	1.03	0.22	0.60
N719:TS	PFN-Br	-5.21	-2.62	PTB7-Th:IEICO-4F	PTB7-Th	-5.22	-3.59	IEICO-4F	-5.44	-4.19	0.720	20.81	58.19	8.72	0	202	48	1.03	0.22	0.60
Ti3C2Tx	PFN-Br	-5.00	-3.90	PBDB-T:ITIC	PBDB-T	-5.52	-3.68	ITIC	-5.70	-4.00	0.910	17.08	70.93	11.02	1	202	49	1.52	0.18	0.32
PEDOT:PSS	PFN-Br	-5.10	-3.90	PBDB-T:ITIC	PBDB-T	-5.52	-3.68	ITIC	-5.70	-4.00	0.900	16.17	66.76	9.72	1	202	49	1.52	0.18	0.32
PEDOT:PSS	PFN-Br	-5.10	-3.90	PM6:Y6	PM6	-5.56	-3.50	Y6	-5.65	-4.10	0.830	24.22	65.16	13.10	1	202	49	1.46	0.09	0.60
Ti3C2Tx	PFN-Br	-5.00	-3.90	PM6:Y6	PM6	-5.56	-3.50	Y6	-5.65	-4.10	0.830	25.63	68.40	14.55	1	202	49	1.46	0.09	0.60
GO/PEDOT:PSS	ZnO	-4.95	-4.20	P3HT:PCBM	P3HT	-5.10	-3.20	PCBM	-6.60	-4.20	0.490	15.42	64.00	4.82	0	201	50	0.90	1.50	1.00
PEDOT:PSS	ZnO	-5.00	-4.20	P3HT:PCBM	P3HT	-5.10	-3.20	PCBM	-6.60	-4.20	0.460	13.38	63.00	4.00	0	201	50	0.90	1.50	1.00
GO	ZnO	-4.90	-4.20	P3HT:PCBM	P3HT	-5.10	-3.20	PCBM	-6.60	-4.20	0.450	11.18	62.00	3.16	0	201	50	0.90	1.50	1.00
PEDOT:PSS	Ca	-5.00	-2.87	PBDB-T:IT-M	PBDB-T	-5.21	-3.41	IT-M	-5.58	-3.98	0.924	15.60	70.50	10.40	1	201	51	1.23	0.37	0.57
MoO3	TiO2	-5.17	-4.14	PBDB-T:IT-M	PBDB-T	-5.21	-3.41	IT-M	-5.58	-3.98	0.923	16.70	70.10	11.20	1	201	51	1.23	0.37	0.57
PEDOT:PSS	PFN	-5.00	-3.85	PTB7:PC71BM	PTB7	-5.20	-3.30	PC71BM	-6.10	-3.90	0.770	15.09	62.30	7.29	0	201	52	1.30	0.90	0.60
F5-rGO	PFN	-5.10	-3.85	PTB7:PC71BM	PTB7	-5.20	-3.30	PC71BM	-6.10	-3.90	0.680	14.78	57.30	5.82	0	201	52	1.30	0.90	0.60
GMo2	TiO2	-4.70	-4.40	PTB7-Th:PC71BM	PTB7-Th	-5.20	-3.60	PC71BM	-6.10	-4.30	0.800	17.10	67.70	9.50	1	201	53	0.90	0.90	0.70
GMo1	TiO2	-4.60	-4.40	PTB7-Th:PC71BM	PTB7-Th	-5.20	-3.60	PC71BM	-6.10	-4.30	0.780	17.80	64.40	9.10	0	201	53	0.90	0.90	0.70
PEDOT:PSS	Ca	-5.10	-2.90	PTB7-Th:PC71BM	PTB7-Th	-5.20	-3.60	PC71BM	-6.10	-4.30	0.770	16.70	67.80	9.00	0	201	53	0.90	0.90	0.70
GMo2	Ca	-4.70	-2.90	PTB7-Th:PC71BM	PTB7-Th	-5.20	-3.60	PC71BM	-6.10	-4.30	0.760	16.10	65.60	8.10	0	201	53	0.90	0.90	0.70
GMo3	TiO2	-5.00	-4.40	PTB7-Th:PC71BM	PTB7-Th	-5.20	-3.60	PC71BM	-6.10	-4.30	0.760	18.90	58.90	8.80	0	201	53	0.90	0.90	0.70
GMo1	Ca	-4.60	-2.90	PTB7-Th:PC71BM	PTB7-Th	-5.20	-3.60	PC71BM	-6.10	-4.30	0.740	15.70	64.80	7.70	0	201	53	0.90	0.90	0.70
GMo3	Ca	-5.00	-2.90	PTB7-Th:PC71BM	PTB7-Th	-5.20	-3.60	PC71BM	-6.10	-4.30	0.740	16.00	63.50	7.40	0	201	53	0.90	0.90	0.70
PEDOT:PSS	PFN-Br	-5.06	-2.70	PM6:Y6	PM6	-5.50	-3.61	Y6	-5.68	-4.06	0.830	26.10	70.00	15.18	1	202	54	1.44	0.18	0.45
PEDOT:PSS:TEMPO+	PFN-Br	-5.03	-2.70	PM6:Y6	PM6	-5.50	-3.61	Y6	-5.68	-4.06	0.830	28.22	67.72	15.78	1	202	54	1.44	0.18	0.45
PEDOT:PSS:TEMPO+	PFN-Br	-5.18	-2.70	PM6:Y6	PM6	-5.50	-3.61	Y6	-5.68	-4.06	0.830	26.98	69.99	15.60	1	202	54	1.44	0.18	0.45
PEDOT:PSS:TEMPO+	PFN-Br	-5.24	-2.70	PM6:Y6	PM6	-5.50	-3.61	Y6	-5.68	-4.06	0.820	26.69	65.62	14.26	1	202	54	1.44	0.18	0.45
PEDOT:PSS:TEMPO+	PFN-Br	-4.96	-2.70	PM6:Y6	PM6	-5.50	-3.61	Y6	-5.68	-4.06	0.810	27.35	71.31	15.90	1	202	54	1.44	0.18	0.45
PMC-4	PFN-Br	-5.40	-2.90	PBDB-T:ITIC	PBDB-T	-5.33	-2.92	ITIC	-5.51	-3.78	0.900	16.80	71.00	10.70	1	202	55	1.21	0.34	0.68
PMC-1	PFN-Br	-5.35	-2.90	PBDB-T-2F:Y6	PBDB-T-2F	-5.31	-3.42	Y6	-5.65	-4.10	0.855	25.50	73.60	16.04	1	202	55	1.21	0.34	0.68
PMC-4	PFN-Br	-5.42	-2.90	PBDB-T-2F:Y6	PBDB-T-2F	-5.31	-3.42	Y6	-5.65	-4.10	0.853	25.48	75.10	16.34	1	202	55	1.21	0.34	0.68
PMC-2	PFN-Br	-5.40	-2.90	PBDB-T-2F:Y6	PBDB-T-2F	-5.31	-3.42	Y6	-5.65	-4.10	0.852	25.26	74.80	16.09	1	202	55	1.21	0.34	0.68
PMC-3	PFN-Br	-5.41	-2.90	PBDB-T-2F:Y6	PBDB-T-2F	-5.31	-3.42	Y6	-5.65	-4.10	0.850	25.42	74.50	16.11	1	202	55	1.21	0.34	0.68
PMC-5	PFN-Br	-5.50	-2.90	PBDB-T-2F:Y6	PBDB-T-2F	-5.31	-3.42	Y6	-5.65	-4.10	0.842	25.16	74.50	15.79	1	202	55	1.21	0.34	0.68
PMC-4	PFN-Br	-5.40	-2.90	PBDB-T-2F:IT-4F	PBDB-T-2F	-5.31	-3.42	IT-4F	-5.65	-4.12	0.840	21.10	75.00	13.20	1	202	55	1.55	0.18	0.86
PEDOT:PSS	PFN-Br	-4.90	-2.90	PBDB-T-2F:Y6	PBDB-T-2F	-5.31	-3.42	Y6	-5.65	-4.10	0.830	25.30	74.80	15.70	1	202	55	1.19	0.34	0.70
MoOx	ZnO/Py-DBP	-6.00	-3.70	PM6:IT-4F	PM6	-5.50	-3.60	IT-4F	-5.86	-4.14	0.820	19.98	72.00	11.80	1	202	56	1.30	0.60	0.30
MoOx	ZnO	-6.00	-4.00	PM6:IT-4F	PM6	-5.50	-3.60	IT-4F	-5.86	-4.14	0.800	19.14	68.00	10.41	1	202	56	1.30	0.60	0.30

MoOx	ZnO/Py-DBP	-6.00	-3.70	PTB7-Th:PC71BM	PTB7-Th	-5.20	-3.60	PC71BM	-5.80	-3.90	0.790	17.83	70.00	9.86	0	202	56	1.36	0.36	0.54
MoOx	ZnO	-6.00	-4.00	PTB7-Th:PC71BM	PTB7-Th	-5.20	-3.60	PC71BM	-5.80	-3.90	0.750	16.19	69.00	8.38	0	202	56	1.36	0.36	0.54
PEDOT:PSS	BCP	-5.10	-3.55	PTB7-Th:PC71BM	PTB7-Th	-5.20	-3.60	PC71BM	-6.10	-4.20	0.815	15.97	65.16	8.48	1	201	57	1.00	0.90	0.60
PEDOT:PSS	PDIN/BCP	-5.10	-3.86	PTB7-Th:PC71BM	PTB7-Th	-5.20	-3.60	PC71BM	-6.10	-4.20	0.815	17.62	70.07	10.05	1	201	57	1.00	0.90	0.60
PEDOT:PSS	PDIN	-5.10	-3.92	PTB7-Th:PC71BM	PTB7-Th	-5.20	-3.60	PC71BM	-6.10	-4.20	0.814	16.50	65.58	8.82	1	201	57	1.00	0.90	0.60
PEDOT:PSS	PFN/BCP	-5.10	-3.86	PTB7-Th:PC71BM	PTB7-Th	-5.20	-3.60	PC71BM	-6.10	-4.20	0.814	17.84	69.55	10.11	1	201	57	1.00	0.90	0.60
PEDOT:PSS	ZrAcac/BCP	-5.10	-3.76	PTB7-Th:PC71BM	PTB7-Th	-5.20	-3.60	PC71BM	-6.10	-4.20	0.814	16.91	70.23	9.66	1	201	57	1.00	0.90	0.60
PEDOT:PSS	ZrAcac	-5.10	-4.41	PTB7-Th:PC71BM	PTB7-Th	-5.20	-3.60	PC71BM	-6.10	-4.20	0.730	15.12	60.25	6.65	0	201	57	1.00	0.90	0.60
PEDOT:PSS	PFN	-5.10	-4.36	PTB7-Th:PC71BM	PTB7-Th	-5.20	-3.60	PC71BM	-6.10	-4.20	0.550	15.85	52.27	4.55	0	201	57	1.00	0.90	0.60
V2O5	ZnO	-4.70	-4.40	PffBT2T-TT:O-IDTBR	PffBT2T-TT	-5.42	-3.52	O-IDTBR	-5.51	-3.55	1.080	14.73	64.00	10.10	1	201	58	1.87	0.09	0.03
V2O5	ZnO	-4.70	-4.40	PffBT2T-TT:PC71BM	PffBT2T-TT	-5.42	-3.52	PC71BM	-6.10	-4.20	0.800	17.71	69.00	9.80	1	201	58	1.22	0.68	0.68
MoO3	ZMO	-5.30	-4.24	PTB7-Th:PC71BM	PTB7-Th	-5.22	-3.64	PC71BM	-6.10	-4.20	0.800	18.40	63.52	9.39	1	201	59	1.02	0.88	0.56
PEDOT:PSS	PHF-N	-5.10	-3.94	PTB7-Th:PC71BM	PTB7-Th	-5.20	-3.60	PC71BM	-6.10	-4.20	0.790	16.16	70.43	8.99	0	201	60	1.00	0.90	0.60
PEDOT:PSS	PHF-BIm4	-5.10	-4.01	PTB7-Th:PC71BM	PTB7-Th	-5.20	-3.60	PC71BM	-6.10	-4.20	0.790	16.22	71.01	9.12	0	201	60	1.00	0.90	0.60
PEDOT:PSS	PCF-Cl	-5.10	-4.21	PTB7-Th:PC71BM	PTB7-Th	-5.20	-3.60	PC71BM	-6.10	-4.20	0.790	16.31	68.41	8.77	0	201	60	1.00	0.90	0.60
PEDOT:PSS	PHF-OH	-5.10	-4.05	PTB7-Th:PC71BM	PTB7-Th	-5.20	-3.60	PC71BM	-6.10	-4.20	0.780	16.96	73.42	9.66	0	201	60	1.00	0.90	0.60
PEDOT:PSS	PHF-F	-5.10	-4.05	PTB7-Th:PC71BM	PTB7-Th	-5.20	-3.60	PC71BM	-6.10	-4.20	0.780	17.10	71.16	9.46	0	201	60	1.00	0.90	0.60
PEDOT:PSS	PCF-N	-5.10	-4.15	PTB7-Th:PC71BM	PTB7-Th	-5.20	-3.60	PC71BM	-6.10	-4.20	0.780	15.98	66.48	8.32	0	201	60	1.00	0.90	0.60
PEDOT:PSS	PCF-BIm4	-5.10	-4.21	PTB7-Th:PC71BM	PTB7-Th	-5.20	-3.60	PC71BM	-6.10	-4.20	0.780	16.10	67.67	8.57	0	201	60	1.00	0.90	0.60
PEDOT:PSS	POF-N	-5.10	-3.82	PTB7-Th:PC71BM	PTB7-Th	-5.20	-3.60	PC71BM	-6.10	-4.20	0.780	16.07	67.84	8.52	0	201	60	1.00	0.90	0.60
PEDOT:PSS	POF-OH	-5.10	-3.86	PTB7-Th:PC71BM	PTB7-Th	-5.20	-3.60	PC71BM	-6.10	-4.20	0.780	17.35	73.74	9.94	0	201	60	1.00	0.90	0.60
PEDOT:PSS	POF-F	-5.10	-3.85	PTB7-Th:PC71BM	PTB7-Th	-5.20	-3.60	PC71BM	-6.10	-4.20	0.780	16.77	71.52	9.34	0	201	60	1.00	0.90	0.60
PEDOT:PSS	PCF-OH	-5.10	-4.22	PTB7-Th:PC71BM	PTB7-Th	-5.20	-3.60	PC71BM	-6.10	-4.20	0.770	15.95	70.17	8.61	0	201	60	1.00	0.90	0.60
PEDOT:PSS	PCF-F	-5.10	-4.22	PTB7-Th:PC71BM	PTB7-Th	-5.20	-3.60	PC71BM	-6.10	-4.20	0.770	17.04	71.83	9.43	0	201	60	1.00	0.90	0.60
PEDOT:PSS	POF-Cl	-5.10	-3.84	PTB7-Th:PC71BM	PTB7-Th	-5.20	-3.60	PC71BM	-6.10	-4.20	0.770	17.12	71.60	9.42	0	201	60	1.00	0.90	0.60
PEDOT:PSS	POF-BIm4	-5.10	-3.85	PTB7-Th:PC71BM	PTB7-Th	-5.20	-3.60	PC71BM	-6.10	-4.20	0.770	16.59	71.22	9.10	0	201	60	1.00	0.90	0.60
PEDOT:PSS	PHF-Cl	-5.10	-4.00	PTB7-Th:PC71BM	PTB7-Th	-5.20	-3.60	PC71BM	-6.10	-4.20	0.750	17.07	66.07	8.49	0	201	60	1.00	0.90	0.60
MoO3	ZnO-PFN	-5.30	-4.26	PTB7:PC71BM	PTB7	-5.22	-3.64	PC71BM	-5.80	-4.00	0.737	18.30	67.80	9.20	0	201	61	1.22	0.58	0.36
MoO3	ZnO	-5.30	-3.86	PTB7:PC71BM	PTB7	-5.22	-3.64	PC71BM	-5.80	-4.00	0.717	16.30	61.70	7.20	0	201	61	1.22	0.58	0.36
MoO3	Ru-TiO2	-5.40	-3.92	PTB7:PC71BM	PTB7	-5.15	-3.31	PC71BM	-6.10	-3.90	0.710	14.64	66.69	6.93	0	201	62	1.25	0.95	0.59
MoO3	An-TiO2	-5.40	-3.87	PTB7:PC71BM	PTB7	-5.15	-3.31	PC71BM	-6.10	-3.90	0.710	15.66	70.63	7.85	0	201	62	1.25	0.95	0.59
MoO3	Am-TiO2	-5.40	-4.33	PTB7:PC71BM	PTB7	-5.15	-3.31	PC71BM	-6.10	-3.90	0.690	13.92	63.57	6.11	0	201	62	1.25	0.95	0.59
MoOx	ZnO:Ba(OH)2	-5.49	-3.94	PTB7-Th:PC70BM	PTB7-Th	-5.22	-3.64	PC70BM	-6.10	-4.30	0.818	15.69	67.60	8.66	1	201	63	0.92	0.88	0.66
MoOx	ZnO/Ba(OH)2	-5.49	-4.23	PTB7-Th:PC70BM	PTB7-Th	-5.22	-3.64	PC70BM	-6.10	-4.30	0.814	15.34	68.20	8.54	1	201	63	0.92	0.88	0.66
MoOx	ZnO	-5.49	-4.36	PTB7-Th:PC70BM	PTB7-Th	-5.22	-3.64	PC70BM	-6.10	-4.30	0.803	14.28	62.30	7.12	1	201	63	0.92	0.88	0.66
MoO3	ZnO:PFN-Br	-6.00	-4.11	PBDB-TF:IT-4F	PBDB-TF	-5.50	-3.61	IT-4F	-5.69	-4.07	0.870	20.16	78.79	13.82	1	201	64	1.43	0.19	0.46
MoO3	ZnO	-6.00	-4.11	PBDB-TF:IT-4F	PBDB-TF	-5.50	-3.61	IT-4F	-5.69	-4.07	0.850	20.13	73.42	12.56	1	201	64	1.43	0.19	0.46
MoO3	PFN-Br	-6.00	-4.17	PBDB-TF:IT-4F	PBDB-TF	-5.50	-3.61	IT-4F	-5.69	-4.07	0.720	17.05	40.73	5.00	0	201	64	1.43	0.19	0.46

MoOx	ZnO:LiF	-5.30	-3.96	P3HT:PC61BM	P3HT	-5.00	-3.10	PC61BM	-6.10	-3.90	0.630	10.38	61.80	4.06	0	201	65	1.10	1.10	0.80
MoOx	ZnO	-5.30	-4.10	P3HT:PC61BM	P3HT	-5.00	-3.10	PC61BM	-6.10	-3.90	0.620	9.03	59.70	3.35	0	201	65	1.10	1.10	0.80
MoOx	ZnO:LiCl	-5.30	-4.06	P3HT:PC61BM	P3HT	-5.00	-3.10	PC61BM	-6.10	-3.90	0.620	9.08	64.00	3.62	0	201	65	1.10	1.10	0.80
MoOx	ZnO:LiBr	-5.30	-4.08	P3HT:PC61BM	P3HT	-5.00	-3.10	PC61BM	-6.10	-3.90	0.610	10.47	59.80	3.85	0	201	65	1.10	1.10	0.80
PEDOT:PSS	PBTA-FN	-5.20	-3.55	PBDB-T-2F:IT-4F	PBDB-T-2F	-5.47	-3.67	IT-4F	-5.69	-4.07	0.880	19.05	72.65	12.18	1	201	66	1.40	0.22	0.40
PEDOT:PSS	PFN	-5.20	-3.69	PBDB-T-2F:IT-4F	PBDB-T-2F	-5.47	-3.67	IT-4F	-5.69	-4.07	0.860	18.15	70.54	11.03	1	201	66	1.40	0.22	0.40
MoO3	SnO2/2Cs2CO3	-5.30	-4.05	P3HT:PC60BM	P3HT	-5.20	-3.30	PC60BM	-6.10	-3.70	0.590	10.29	57.62	3.50	0	201	67	1.50	0.90	0.40
MoO3	SnO2/1Cs2CO3	-5.30	-4.16	P3HT:PC60BM	P3HT	-5.20	-3.30	PC60BM	-6.10	-3.70	0.580	10.58	59.91	3.69	0	201	67	1.50	0.90	0.40
MoO3	SnO2/3Cs2CO3	-5.30	-3.92	P3HT:PC60BM	P3HT	-5.20	-3.30	PC60BM	-6.10	-3.70	0.580	8.18	47.34	2.24	0	201	67	1.50	0.90	0.40
MoO3	SnO2	-5.30	-4.34	P3HT:PC60BM	P3HT	-5.20	-3.30	PC60BM	-6.10	-3.70	0.550	10.16	47.83	2.68	0	201	67	1.50	0.90	0.40
MoO3	ZnO	-5.30	-4.11	PTB7-Th:PC71BM	PTB7-Th	-5.22	-3.64	PC71BM	-5.87	-3.91	0.790	16.88	68.00	9.07	0	201	68	1.31	0.65	0.27
MoO3	ZnO:PEI	-5.30	-4.04	PTB7-Th:PC71BM	PTB7-Th	-5.22	-3.64	PC71BM	-5.87	-3.91	0.790	16.87	68.00	9.06	0	201	68	1.31	0.65	0.27
MoO3	Bilayer	-5.60	-4.04	PBDB-T:ITIC	PBDB-T	-5.33	-2.92	ITIC	-5.96	-3.98	0.936	19.42	65.30	11.87	1	201	69	1.35	0.63	1.06
MoO3	ZnO-NP	-5.60	-4.04	PBDB-T:ITIC	PBDB-T	-5.33	-2.92	ITIC	-5.96	-3.98	0.932	17.97	66.20	11.10	1	201	69	1.35	0.63	1.06
MoO3	DZO	-5.60	-4.08	PBDB-T:ITIC	PBDB-T	-5.33	-2.92	ITIC	-5.96	-3.98	0.925	18.87	63.30	11.06	1	201	69	1.35	0.63	1.06
MoO3	ZnO	-5.60	-4.16	PBDB-T:ITIC	PBDB-T	-5.33	-2.92	ITIC	-5.96	-3.98	0.924	18.64	61.10	10.53	1	201	69	1.35	0.63	1.06
MoOx	TiO2/B2-W	-6.00	-4.00	P3HT:IC60BA	P3HT	-5.10	-3.30	IC60BA	-5.70	-3.70	0.810	10.60	70.00	6.01	1	201	70	1.40	0.60	0.40
MoOx	TiO2/B1-Mo	-6.00	-3.80	P3HT:IC60BA	P3HT	-5.10	-3.30	IC60BA	-5.70	-3.70	0.810	10.80	71.00	6.21	1	201	70	1.40	0.60	0.40
MoOx	TiO2/B1-W	-6.00	-4.20	P3HT:IC60BA	P3HT	-5.10	-3.30	IC60BA	-5.70	-3.70	0.800	10.40	69.00	5.74	1	201	70	1.40	0.60	0.40
MoOx	TiO2	-6.00	-4.50	P3HT:IC60BA	P3HT	-5.10	-3.30	IC60BA	-5.70	-3.70	0.770	9.90	65.00	4.95	0	201	70	1.40	0.60	0.40
MoOx	TiO2/B2-W	-6.00	-4.00	PTB7:PC70BM	PTB7	-5.20	-3.20	PC70BM	-5.90	-3.90	0.750	15.40	68.00	7.85	0	201	70	1.30	0.70	0.70
MoOx	TiO2/B1-Mo	-6.00	-3.80	PTB7:PC70BM	PTB7	-5.20	-3.20	PC70BM	-5.90	-3.90	0.750	15.60	69.00	8.07	0	201	70	1.30	0.70	0.70
MoOx	TiO2/B1-W	-6.00	-4.20	PTB7:PC70BM	PTB7	-5.20	-3.20	PC70BM	-5.90	-3.90	0.740	14.90	66.00	7.28	0	201	70	1.30	0.70	0.70
MoOx	TiO2	-6.00	-4.50	PTB7:PC70BM	PTB7	-5.20	-3.20	PC70BM	-5.90	-3.90	0.710	14.40	65.00	6.65	0	201	70	1.30	0.70	0.70
PEDOT:PSS	PDIN	-5.20	-4.56	PM6:Y6	PM6	-5.54	-3.61	Y6	-5.62	-4.11	0.854	25.64	70.38	15.24	1	202	71	1.43	0.08	0.50
PEDOT:PSS	PDIN/DMeKL	-5.20	-4.34	PM6:Y6	PM6	-5.54	-3.61	Y6	-5.62	-4.11	0.849	26.61	70.89	15.96	1	202	71	1.43	0.08	0.50
PEDOT:PSS	DMeKL	-5.20	-3.92	PM6:Y6	PM6	-5.54	-3.61	Y6	-5.62	-4.11	0.724	11.77	49.63	4.03	0	202	71	1.43	0.08	0.50
PEDOT:PSS	PDINN	-5.10	-3.72	J11:m-ITTC	J11	-5.48	-3.23	m-ITTC	-5.62	-3.89	0.934	18.68	70.02	12.21	1	202	72	1.46	0.09	0.60
PEDOT:PSS	PDINN	-5.10	-3.72	PTQ10:IT-4F	PTQ10	-5.54	-2.98	IT-4F	-5.74	-3.90	0.929	19.97	72.24	13.40	1	202	72	1.46	0.09	0.60
PEDOT:PSS	PDINO	-5.10	-3.88	J11:m-ITTC	J11	-5.48	-3.23	m-ITTC	-5.62	-3.89	0.914	18.37	66.30	11.13	1	202	72	1.64	0.20	0.92
PEDOT:PSS	PDINO	-5.10	-3.88	PTQ10:IT-4F	PTQ10	-5.54	-2.98	IT-4F	-5.74	-3.90	0.899	19.47	67.60	11.83	1	202	72	1.64	0.20	0.92
PEDOT:PSS	PDINN	-5.10	-3.72	PM6:Y6	PM6	-5.56	-3.50	Y6	-5.65	-4.10	0.847	25.89	78.59	17.23	1	202	72	1.59	0.14	0.66
PEDOT:PSS	PDINO	-5.10	-3.88	PM6:Y6	PM6	-5.56	-3.50	Y6	-5.65	-4.10	0.821	25.58	72.24	15.17	1	202	72	1.59	0.14	0.66
PEDOT:PSS	ZnO	-5.20	-4.10	P3HT:PCBM	P3HT	-5.30	-3.10	PCBM	-6.10	-3.80	0.550	4.51	31.00	0.80	0	202	73	1.50	0.80	0.70
PEDOT:PSS	ZnO:PEIE	-5.20	-4.30	P3HT:PCBM	P3HT	-5.30	-3.10	PCBM	-6.10	-3.80	0.540	4.73	37.00	0.95	0	202	73	1.50	0.80	0.70
MoO3	TiO2:TOPD	-5.40	-4.23	PTB7-Th:PC71BM	PTB7-Th	-5.12	-3.60	PC71BM	-6.00	-4.30	0.800	18.09	67.80	9.82	1	201	74	0.82	0.88	0.70
MoO3	TiO2:TOPD-UE	-5.40	-4.14	PTB7-Th:PC71BM	PTB7-Th	-5.12	-3.60	PC71BM	-6.00	-4.30	0.790	18.84	70.85	10.55	0	201	74	0.82	0.88	0.70
MoO3	TiO2	-5.40	-4.43	PTB7-Th:PC71BM	PTB7-Th	-5.12	-3.60	PC71BM	-6.00	-4.30	0.770	18.13	62.24	8.73	0	201	74	0.82	0.88	0.70

MoO3	ZnO:PEIE:RGO	-5.30	-4.25	PTB7:PCBM	PTB7	-5.15	-3.31	PCBM	-6.00	-4.10	0.790	15.95	70.40	8.87	0	201	75	1.05	0.85	0.79
MoO3	ZnO	-5.30	-4.23	PTB7:PCBM	PTB7	-5.15	-3.31	PCBM	-6.00	-4.10	0.780	14.28	62.00	6.91	0	201	75	1.05	0.85	0.79
PEDOT:PSS	PDINO	-5.10	-3.63	J12:m-ITTC	J12	-5.51	-3.26	m-ITTC	-5.62	-3.89	0.943	16.64	55.70	8.74	1	201	76	1.59	0.14	0.66
PEDOT:PSS	PDINO	-5.10	-3.63	J11:m-ITTC	J11	-5.48	-3.23	m-ITTC	-5.62	-3.89	0.935	18.05	73.00	12.32	1	201	76	1.62	0.11	0.63
MoO3	SnO2/PeNWs	-5.30	-3.90	PBDB-T-SF:IT-4F	PBDB-T-SF	-5.40	-3.60	IT-4F	-5.66	-4.14	0.819	23.92	54.70	10.72	1	202	77	1.26	0.26	0.54
MoO3	SnO2	-5.30	-3.65	PBDB-T-SF:IT-4F	PBDB-T-SF	-5.40	-3.60	IT-4F	-5.66	-4.14	0.786	22.39	54.10	9.53	0	202	77	1.26	0.26	0.54
PH1000	PFN-Br	-4.90	-3.63	PM6:Y6	PM6	-5.45	-3.65	Y6	-5.65	-4.10	0.837	19.12	70.60	11.30	1	201	78	1.35	0.20	0.45
PH1000	PFN-Br	-4.90	-3.63	PM6:IT-4F	PM6	-5.45	-3.65	IT-4F	-5.66	-4.14	0.835	22.46	71.85	13.48	1	201	78	1.31	0.21	0.49
PEDOT:PSS:5WS2NS	PDINN	-5.30	-3.78	PM6:Y6	PM6	-5.50	-3.56	Y6	-5.70	-4.10	0.835	25.32	73.49	15.52	1	202	79	1.40	0.20	0.54
PEDOT:PSS:3WS2NS	PDINN	-5.27	-3.78	PM6:Y6	PM6	-5.50	-3.56	Y6	-5.70	-4.10	0.834	25.55	73.50	15.69	1	202	79	1.40	0.20	0.54
PEDOT:PSS	PDINN	-5.00	-3.78	PM6:Y6	PM6	-5.50	-3.56	Y6	-5.70	-4.10	0.833	24.08	71.48	14.35	1	202	79	1.40	0.20	0.54
PEDOT:PSS:1WS2NS	PDINN	-5.15	-3.78	PM6:Y6	PM6	-5.50	-3.56	Y6	-5.70	-4.10	0.832	25.20	72.97	15.31	1	202	79	1.40	0.20	0.54
PPy-PEDOT:PSS	Ca	-5.16	-2.80	PTB7:PC71BM	PTB7	-5.15	-3.31	PC71BM	-6.00	-4.00	0.760	17.55	71.06	9.48	0	201	80	1.20	0.80	0.70
PPy-PEDOT:PSS	Ca	-5.16	-2.80	P3HT:PC71BM	P3HT	-5.20	-3.30	PC71BM	-6.00	-4.00	0.550	9.09	67.93	3.40	0	201	80	1.15	0.85	0.69
PEDOT:PSS:0.15-	PFN-Br	-5.06	-3.90	PBDB-T:ITIC	PBDB-T	-5.52	-3.68	ITIC	-5.70	-4.00	0.910	17.31	71.14	11.22	1	202	81	1.52	0.18	0.32
PEDOT:PSS	PFN-Br	-5.10	-3.90	PBDB-T:ITIC	PBDB-T	-5.52	-3.68	ITIC	-5.70	-4.00	0.900	16.23	69.91	10.21	1	202	81	1.52	0.18	0.32
PEDOT:PSS:0.20-	PFN-Br	-5.03	-3.90	PBDB-T:ITIC	PBDB-T	-5.52	-3.68	ITIC	-5.70	-4.00	0.900	16.65	70.56	10.62	1	202	81	1.52	0.18	0.32
PEDOT:PSS	PF6NPSBr:10Cs2CO3	-5.10	-3.90	PTB7-Th:PC71BM	PTB7-Th	-5.20	-3.59	PC71BM	-5.87	-3.91	0.783	15.10	71.18	8.52	0	201	82	1.29	0.67	0.32
PEDOT:PSS	PF6NPSBr:15Cs2CO3	-5.10	-3.85	PTB7-Th:PC71BM	PTB7-Th	-5.20	-3.59	PC71BM	-5.87	-3.91	0.764	13.43	47.15	4.90	0	201	82	1.29	0.67	0.32
PEDOT:PSS	PF6NPSBr:05Cs2CO3	-5.10	-4.11	PTB7-Th:PC71BM	PTB7-Th	-5.20	-3.59	PC71BM	-5.87	-3.91	0.760	14.85	65.32	7.39	0	201	82	1.29	0.67	0.32
PEDOT:PSS	PF6NPSBr	-5.10	-4.20	PTB7-Th:PC71BM	PTB7-Th	-5.20	-3.59	PC71BM	-5.87	-3.91	0.743	14.83	62.44	6.97	0	201	82	1.29	0.67	0.32
PEDOT:PSS	QPhPBr	-5.10	-3.95	PTB7-Th:PC71BM	PTB7-Th	-5.17	-3.59	PC71BM	-5.87	-3.91	0.815	16.78	67.12	9.18	1	201	83	1.26	0.70	0.32
PEDOT:PSS	N719:QPhPBr	-5.10	-3.93	PTB7-Th:PC71BM	PTB7-Th	-5.17	-3.59	PC71BM	-5.87	-3.91	0.814	17.26	69.96	9.83	1	201	83	1.26	0.70	0.32
PEDOT:PSS	N719	-5.10	-3.16	PTB7-Th:PC71BM	PTB7-Th	-5.17	-3.59	PC71BM	-5.87	-3.91	0.803	16.34	65.41	8.58	1	201	83	1.26	0.70	0.32
PEDOT:PSS	QPhPBr	-5.10	-3.95	PBDTTT-CT:PC71BM	PBDTTT-CT	-5.11	-3.25	PC71BM	-5.87	-3.91	0.771	16.64	65.68	8.42	0	201	83	1.20	0.76	0.66
PEDOT:PSS	N719:QPhPBr	-5.10	-3.93	PBDTTT-CT:PC71BM	PBDTTT-CT	-5.11	-3.25	PC71BM	-5.87	-3.91	0.770	17.01	66.22	8.69	0	201	83	1.20	0.76	0.66
PEDOT:PSS	N719	-5.10	-3.16	PBDTTT-CT:PC71BM	PBDTTT-CT	-5.11	-3.25	PC71BM	-5.87	-3.91	0.752	15.52	65.23	7.61	0	201	83	1.20	0.76	0.66
MoO3	ZnO	-5.30	-4.40	PTB7-Th:PC71BM	PTB7-Th	-5.20	-3.60	PC71BM	-6.10	-3.90	0.780	16.81	67.51	8.89	0	201	84	1.30	0.90	0.30
MoO3	PCBB-N-I	-5.30	-4.07	PTB7-Th:PC71BM	PTB7-Th	-5.20	-3.60	PC71BM	-6.10	-3.90	0.780	17.12	63.35	8.45	0	201	84	1.30	0.90	0.30
MoO3	PCBB-3N-3I	-5.30	-4.00	PTB7-Th:PC71BM	PTB7-Th	-5.20	-3.60	PC71BM	-6.10	-3.90	0.780	19.68	69.10	10.62	0	201	84	1.30	0.90	0.30
MoO3	ZnO	-5.00	-4.20	PBDB-T:ITIC	PBDB-T	-5.52	-3.68	ITIC	-5.70	-4.00	0.900	16.91	67.80	10.32	1	202	85	1.52	0.18	0.32
MoO3	ZnO:0.03GHK-Cu	-5.00	-4.19	PBDB-T:ITIC	PBDB-T	-5.52	-3.68	ITIC	-5.70	-4.00	0.900	17.44	68.80	10.80	1	202	85	1.52	0.18	0.32
MoO3	ZnO:0.05GHK-Cu	-5.00	-4.18	PBDB-T:ITIC	PBDB-T	-5.52	-3.68	ITIC	-5.70	-4.00	0.900	18.10	70.60	11.50	1	202	85	1.52	0.18	0.32
MoO3	ZnO:0.10GHK-Cu	-5.00	-4.17	PBDB-T:ITIC	PBDB-T	-5.52	-3.68	ITIC	-5.70	-4.00	0.900	18.33	72.30	11.93	1	202	85	1.52	0.18	0.32
MoO3	ZnO:0.30GHK-Cu	-5.00	-4.15	PBDB-T:ITIC	PBDB-T	-5.52	-3.68	ITIC	-5.70	-4.00	0.900	17.93	69.70	11.25	1	202	85	1.52	0.18	0.32
L-GO	ZnO	-4.98	-4.40	PTB7-Th:PC71BM	PTB7-Th	-5.22	-3.64	PC71BM	-5.80	-4.00	0.780	18.39	61.00	8.80	0	201	86	1.22	0.58	0.36
L-GO:NiOx	ZnO	-4.97	-4.40	PTB7-Th:PC71BM	PTB7-Th	-5.22	-3.64	PC71BM	-5.80	-4.00	0.780	19.16	65.00	9.73	0	201	86	1.22	0.58	0.36
NiOx	ZnO	-4.76	-4.40	PTB7-Th:PC71BM	PTB7-Th	-5.22	-3.64	PC71BM	-5.80	-4.00	0.570	17.63	55.00	5.52	0	201	86	1.22	0.58	0.36

MoOx	TSi/sg-ZnO	-5.30	-4.21	PBDFP-Bz:Y6	PBDFP-Bz	-5.50	-3.46	Y6	-5.65	-4.10	0.841	25.14	77.42	16.37	1	202	87	1.40	0.15	0.64
MoOx	sg-ZnO	-5.30	-4.45	PBDFP-Bz:Y6	PBDFP-Bz	-5.50	-3.46	Y6	-5.65	-4.10	0.822	24.39	75.30	15.10	1	202	87	1.40	0.15	0.64
PEDOT:PSS	ZnO	-5.23	-4.20	PTB7-Th:PC71BM	PTB7-Th	-5.30	-3.80	PC71BM	-5.90	-3.90	0.793	15.49	70.12	8.62	0	201	88	1.40	0.60	0.10
PEDOT:PSS/TTF-py	ZnO	-5.29	-4.20	PTB7-Th:PC71BM	PTB7-Th	-5.30	-3.80	PC71BM	-5.90	-3.90	0.790	17.19	70.57	9.58	0	201	88	1.40	0.60	0.10
MoOx/BPQD2	ZnO/BPQD1	-5.12	-4.21	PTB7-Th:FOIC	PTB7-Th	-5.20	-3.56	FOIC	-5.36	-3.92	0.724	25.80	70.50	13.10	0	201	89	1.28	0.16	0.36
MoOx	ZnO/BPQD1	-5.30	-4.21	PTB7-Th:FOIC	PTB7-Th	-5.20	-3.56	FOIC	-5.36	-3.92	0.715	25.60	69.60	12.70	0	201	89	1.28	0.16	0.36
MoOx/BPQD2	ZnO	-5.12	-4.30	PTB7-Th:FOIC	PTB7-Th	-5.20	-3.56	FOIC	-5.36	-3.92	0.715	25.30	69.10	12.40	0	201	89	1.28	0.16	0.36
MoOx	ZnO	-5.30	-4.30	PTB7-Th:FOIC	PTB7-Th	-5.20	-3.56	FOIC	-5.36	-3.92	0.711	24.10	68.90	11.80	0	201	89	1.28	0.16	0.36
TTA	ZnO	-5.26	-4.20	PTB7-Th:PC71BM	PTB7-Th	-5.30	-3.80	PC71BM	-5.90	-3.90	0.794	15.95	69.21	9.09	0	201	90	1.40	0.60	0.10
PEDOT:PSS	ZnO	-5.10	-4.20	PTB7-Th:PC71BM	PTB7-Th	-5.30	-3.80	PC71BM	-5.90	-3.90	0.789	15.46	68.59	8.61	0	201	90	1.40	0.60	0.10
MoO3	CD:2.0ZnO	-5.60	-3.92	PM6:IT-4F	PM6	-5.45	-3.65	IT-4F	-5.66	-4.14	0.830	20.75	71.00	12.23	1	202	91	1.31	0.21	0.49
MoO3	CD:0.5ZnO	-5.60	-3.97	PM6:IT-4F	PM6	-5.45	-3.65	IT-4F	-5.66	-4.14	0.820	20.32	72.00	12.00	1	202	91	1.31	0.21	0.49
MoO3	CD:1.0ZnO	-5.60	-3.92	PM6:IT-4F	PM6	-5.45	-3.65	IT-4F	-5.66	-4.14	0.820	20.90	70.00	12.01	1	202	91	1.31	0.21	0.49
MoO3	ZnO	-5.60	-4.04	PM6:IT-4F	PM6	-5.45	-3.65	IT-4F	-5.66	-4.14	0.810	20.44	68.00	11.26	1	202	91	1.31	0.21	0.49
MoO3	CD:3.0ZnO	-5.60	-4.01	PM6:IT-4F	PM6	-5.45	-3.65	IT-4F	-5.66	-4.14	0.800	21.21	63.00	10.69	1	202	91	1.31	0.21	0.49
MoO3	HfACBV4	-5.40	-3.90	PM6:Y6	PM6	-5.40	-3.65	Y6	-5.65	-4.10	0.820	25.27	71.01	14.61	1	202	92	1.30	0.25	0.45
MoO3	ACBV	-5.40	-3.81	PM6:Y6	PM6	-5.40	-3.65	Y6	-5.65	-4.10	0.770	24.11	62.07	11.37	0	202	92	1.30	0.25	0.45
MoO3	ZnO/TCNE	-5.40	-4.04	PTB7:PC71BM	PTB7	-5.25	-3.13	PC71BM	-5.90	-3.90	0.760	18.60	64.20	8.59	0	202	93	1.35	0.65	0.77
MoO3	ZnO	-5.40	-4.14	PTB7:PC71BM	PTB7	-5.25	-3.13	PC71BM	-5.90	-3.90	0.730	16.20	57.60	7.47	0	202	93	1.35	0.65	0.77
PEDOT:PSS	PFN-Br	-5.10	-3.90	PBDB-T:ITIC	PBDB-T	-5.52	-3.68	ITIC	-5.70	-4.00	0.900	16.14	69.59	10.11	1	201	94	1.52	0.18	0.32
Ti3C2Tx	PFN-Br	-5.00	-3.90	PBDB-T:ITIC	PBDB-T	-5.52	-3.68	ITIC	-5.70	-4.00	0.880	17.85	67.06	10.53	1	201	94	1.52	0.18	0.32
PEDOT:PSS	BIPO	-5.00	-3.82	PTB7:PC71BM	PTB7	-5.20	-3.30	PC71BM	-5.90	-3.90	0.730	16.17	59.00	7.63	0	202	95	1.30	0.70	0.60
PEDOT:PSS	TIPO	-5.00	-4.04	PTB7:PC71BM	PTB7	-5.20	-3.30	PC71BM	-5.90	-3.90	0.700	15.82	58.00	7.04	0	202	95	1.30	0.70	0.60
PEDOT:PSS	P3P-NBr	-5.10	-3.84	J71:ITIC	J71	-5.40	-3.24	ITIC	-5.51	-3.84	0.941	16.47	67.48	10.46	1	201	96	1.56	0.11	0.60
PEDOT:PSS	P1P-NO	-5.10	-3.72	J71:ITIC	J71	-5.40	-3.24	ITIC	-5.51	-3.84	0.940	17.47	70.35	11.56	1	201	96	1.56	0.11	0.60
PEDOT:PSS	P4P-NBr	-5.10	-3.60	J71:ITIC	J71	-5.40	-3.24	ITIC	-5.51	-3.84	0.939	16.45	55.28	8.54	1	201	96	1.56	0.11	0.60
PEDOT:PSS	P2P-NBr	-5.10	-3.58	J71:ITIC	J71	-5.40	-3.24	ITIC	-5.51	-3.84	0.938	16.08	65.50	9.90	1	201	96	1.56	0.11	0.60
PEDOT:PSS	PDI-NBr	-5.10	-3.79	J71:ITIC	J71	-5.40	-3.24	ITIC	-5.51	-3.84	0.936	15.85	48.14	7.14	1	201	96	1.56	0.11	0.60
PEDOT:PSS	PDI-NO	-5.10	-3.59	J71:ITIC	J71	-5.40	-3.24	ITIC	-5.51	-3.84	0.935	17.14	69.19	11.09	1	201	96	1.56	0.11	0.60
PEDOT:PSS	P2P-NO	-5.10	-3.75	J71:ITIC	J71	-5.40	-3.24	ITIC	-5.51	-3.84	0.934	17.38	65.26	10.60	1	201	96	1.56	0.11	0.60
PEDOT:PSS	P1P-NBr	-5.10	-3.70	J71:ITIC	J71	-5.40	-3.24	ITIC	-5.51	-3.84	0.929	16.05	58.71	8.76	1	201	96	1.56	0.11	0.60
PEDOT:PSS	P3P-NO	-5.10	-3.70	J71:ITIC	J71	-5.40	-3.24	ITIC	-5.51	-3.84	0.926	17.11	64.81	10.27	1	201	96	1.56	0.11	0.60
PEDOT:PSS	P4P-NO	-5.10	-3.69	J71:ITIC	J71	-5.40	-3.24	ITIC	-5.51	-3.84	0.917	16.21	65.24	9.60	1	201	96	1.56	0.11	0.60
PEDOT:PSS	3FPy	-5.20	-4.33	PTB7:PC71BM	PTB7	-5.20	-3.30	PC71BM	-5.90	-3.90	0.750	15.40	62.00	7.16	0	202	97	1.30	0.70	0.60
PEDOT:PSS	MeOH	-5.20	-4.80	PTB7:PC71BM	PTB7	-5.20	-3.30	PC71BM	-5.90	-3.90	0.640	15.50	55.10	5.47	0	202	97	1.30	0.70	0.60
MoOx	PBSON-P	-5.30	-4.65	PTB7-Th:PC71BM	PTB7-Th	-5.30	-3.70	PC71BM	-5.90	-3.90	0.780	17.02	69.55	9.32	0	201	98	1.40	0.60	0.20
MoOx	PBSON-FEO	-5.30	-4.58	PTB7-Th:PC71BM	PTB7-Th	-5.30	-3.70	PC71BM	-5.90	-3.90	0.780	17.06	70.28	9.58	0	201	98	1.40	0.60	0.20
PEDOT:PSS	PBSON-P	-5.20	-4.65	PTB7-Th:PC71BM	PTB7-Th	-5.30	-3.70	PC71BM	-5.90	-3.90	0.780	16.28	70.18	9.08	0	201	98	1.40	0.60	0.20

PEDOT:PSS	PBSON-FEO	-5.20	-4.58	PTB7-Th:PC71BM	PTB7-Th	-5.30	-3.70	PC71BM	-5.90	-3.90	0.780	16.24	70.66	9.10	0	201	98	1.40	0.60	0.20
MoOx	ZnO	-5.60	-3.77	PBDB-T:ITIC-M	PBDB-T	-5.30	-3.50	ITIC-M	-5.40	-3.80	0.930	18.09	70.00	11.76	1	202	99	1.50	0.10	0.30
MoOx	PEIE-EDT	-5.60	-3.70	PBDB-T:ITIC-M	PBDB-T	-5.30	-3.50	ITIC-M	-5.40	-3.80	0.920	19.16	69.00	12.06	1	202	99	1.50	0.10	0.30
MoOx	PEIE	-5.60	-3.90	PBDB-T:ITIC-M	PBDB-T	-5.30	-3.50	ITIC-M	-5.40	-3.80	0.860	18.92	59.00	9.60	1	202	99	1.50	0.10	0.30
MoO3	LA-PEIE	-5.20	-4.10	PTB7-Th:PC70BM	PTB7-Th	-5.30	-3.70	PC70BM	-6.10	-4.20	0.820	19.33	68.00	10.57	1	202	100	1.10	0.80	0.50
MoO3	ZnO	-5.20	-4.30	PTB7-Th:PC70BM	PTB7-Th	-5.30	-3.70	PC70BM	-6.10	-4.20	0.800	18.63	67.00	9.46	1	202	100	1.10	0.80	0.50
MoO3	PEIE	-5.20	-4.40	PTB7-Th:PC70BM	PTB7-Th	-5.30	-3.70	PC70BM	-6.10	-4.20	0.800	17.73	66.00	9.30	1	202	100	1.10	0.80	0.50
MoO3	PCBM:5.0TMHT	-6.70	-4.40	PM6:IT-4F	PM6	-5.50	-3.70	IT-4F	-5.70	-4.00	0.840	19.83	69.00	11.41	1	202	101	1.50	0.20	0.30
MoO3	PCBM:2.0TMHT	-6.70	-4.50	PM6:IT-4F	PM6	-5.50	-3.70	IT-4F	-5.70	-4.00	0.800	18.98	57.00	8.65	1	202	101	1.50	0.20	0.30
MoO3	PCBM:0.1TMHT	-6.70	-4.60	PM6:IT-4F	PM6	-5.50	-3.70	IT-4F	-5.70	-4.00	0.720	13.97	25.00	2.51	0	202	101	1.50	0.20	0.30
CuSCN	BCP	-5.56	-3.50	PM6:Y6	PM6	-5.50	-3.61	Y6	-5.65	-4.10	0.850	22.07	70.10	13.13	1	202	102	1.40	0.15	0.49
CuSCN:TFB	BCP	-5.50	-3.50	PM6:Y6	PM6	-5.50	-3.61	Y6	-5.65	-4.10	0.850	24.35	73.84	15.28	1	202	102	1.40	0.15	0.49
PFS	PFSF	-5.15	-2.95	PBDB-T:IT-M	PBDB-T	-5.15	-3.41	IT-M	-5.58	-3.85	0.893	16.90	67.00	10.20	1	201	103	1.30	0.43	0.44
PFS	PFS	-5.15	-2.80	PBDB-T:IT-M	PBDB-T	-5.15	-3.41	IT-M	-5.58	-3.85	0.871	16.90	65.00	9.54	1	201	103	1.30	0.43	0.44
PFSF	PFSF	-5.34	-2.95	PBDB-T:IT-M	PBDB-T	-5.15	-3.41	IT-M	-5.58	-3.85	0.836	16.20	44.00	5.89	1	201	103	1.30	0.43	0.44
PFB	PFB	-5.70	-2.77	PBDB-T:IT-M	PBDB-T	-5.15	-3.41	IT-M	-5.58	-3.85	0.768	14.00	17.00	1.80	0	201	103	1.30	0.43	0.44
MoOx	ZnO:Li	-5.30	-4.02	PTB7-Th:IT-4F	PTB7-Th	-5.40	-3.80	IT-4F	-5.66	-4.14	0.830	16.12	67.00	8.96	1	201	104	1.40	0.50	0.20
MoOx	ZnO:Li	-5.30	-4.02	PTB7-Th:PC71BM	PTB7-Th	-5.40	-3.80	PC71BM	-5.90	-4.00	0.800	17.94	70.00	10.05	1	201	104	1.40	0.50	0.20
MoOx	ZnO	-5.30	-3.95	PTB7-Th:IT-4F	PTB7-Th	-5.40	-3.80	IT-4F	-5.66	-4.14	0.790	15.02	63.00	7.47	0	201	104	1.26	0.26	0.34
MoOx	ZnO	-5.30	-3.95	PTB7-Th:PC71BM	PTB7-Th	-5.40	-3.80	PC71BM	-5.90	-4.00	0.760	16.62	68.00	8.59	0	201	104	1.26	0.26	0.34
PEDOT:PSS@PWA	PDIN	-5.48	-3.72	PM6:Y6	PM6	-5.48	-3.61	Y6	-5.65	-4.10	0.867	25.70	76.30	16.90	1	202	105	1.38	0.17	0.49
PEDOT:PSS	PDIN	-5.30	-3.72	PM6:Y6	PM6	-5.48	-3.61	Y6	-5.65	-4.10	0.854	24.70	74.80	15.60	1	202	105	1.38	0.17	0.49
PEDOT:PSS	PDINO	-5.10	-3.63	BTEC-2F:Y6	BTEC-2F	-5.39	-3.38	Y6	-5.65	-4.10	0.854	21.55	72.35	13.34	1	202	106	1.29	0.26	0.72
PEDOT:PSS	PDINO	-5.10	-3.63	BT-2F:Y6	BT-2F	-5.40	-3.40	Y6	-5.65	-4.10	0.853	22.38	72.27	13.80	1	202	106	1.30	0.25	0.70

Table S2. The energy level/work function values of the materials in OSCs from the literature.

Materials	Energy levels		Ref
PTB7	-5.15	-3.31	112
PTB7-Th	-5.24	-3.62	112
PffBT4T-2OD	-5.34	-3.69	113
PM6	-5.50	-3.61	114
$PC_{71}BM$	-6.10	-3.90	112
Y6	-5.65	-4.10	114
ITIC-M	-5.58	-3.98	115
PEDOT:PSS	-5.10		116
PDINO	-3.63		116
MoOx	-5.60		117
ZnO	-4.40		117

Table S3. Device characteristics of the organic solar cells using the same structure in literature. And the relative error (%) between the predicted values of V_{oc} based on XGBoost model and measured V_{oc} in literature, which is calculated as = $[(V_{oc\ predicted} - V_{oc\ measured})/ V_{oc\ measured}]$*%.

Ref	V_{oc} (V)	Relative error (%)	Active layer	J_{sc} (mA/cm^2	FF (%)	PCE (%)	HTL	ETL
118	0.73	8.22%	$PTB7:PC_{71}BM_{(CF)}$	18.52	66.0	8.95	PEDOT:PS	LiF
	0.75	5.33%	$PTB7:PC_{71}BM_{(O-CB)}$	15.98	66.0	7.97	PEDOT:PS	LiF
	0.74	6.75%	$PTB7:PC_{71}BM_{(CB)}$	19.64	67.0	9.64	PEDOT:PS	LiF
119	0.80	0%	$PTB7\text{-}Th:PC_{71}BM$	12.92	44.0	4.58	PEDOT:PS	LiF
120	0.79	1.27%	$PTB7\text{-}Th:PC_{71}BM$	20.70	59.0	9.80	PEDOT:PS	LiF
	0.78	2.56%	$PTB7\text{-}Th:PC_{71}BM_{(1:1.2)}$	16.90	54.0	7.20	PEDOT:PS	LiF
121	0.74	5.76%	$PTB7:PC_{71}BM$	16.06	69.6	8.36	PEDOT:PS	LiF
122	0.78	5.13%	$PffBT4T\text{-}2OD:PC_{71}BM$	15.896	64.4	8.08	PEDOT:PS	LiF
	0.78	5.13%	$PffBT4T\text{-}2OD:PC_{71}BM_{(ODT)}$	15.993	61.9	7.72	PEDOT:PS	LiF
	0.79	3.80%	$PffBT4T\text{-}2OD:PC_{71}BM_{(DIO)}$	16.785	66.4	8.91	PEDOT:PS	LiF
	0.78	5.13%	$PffBT4T\text{-}2OD:PC_{71}BM_{(DPE)}$	17.304	69.0	9.31	PEDOT:PS	LiF
	0.79	3.80%	$PffBT4T\text{-}2OD:PC_{71}BM_{(CN)}$	17.752	73.1	10.2	PEDOT:PS	LiF
123	0.71	5.63%	$PTB7:PC_{71}BM_{(DIO)}$	14.50	67.1	6.96	MoO_3	ZnO
	0.70	7.14%	$PTB7:PC_{71}BM_{(DPE)}$	14.80	64.6	6.69	MoO_3	ZnO
	0.72	4.17%	$PTB7:PC_{71}BM_{(DIO+DPE)}$	18.10	71.0	9.25	MoO_3	ZnO
124	0.74	1.35%	$PTB7:PC_{70}BM$	13.20	65.4	6.44	MoO_x	ZnO
	0.77	6.49%	$PffBT4T\text{-}2OD:PC_{70}BM$	17.90	66.0	9.16	MoO_x	ZnO
125	0.78	2.56%	$PTB7\text{-}Th:PC_{71}BM$	17.88	66.0	9.30	MoO_3	ZnO
126	0.74	1.35%	PTB7:PCBM	15.00	70.0	7.80	MoO_3	ZnO
	0.80	0%	PTB7-Th:PCBM	15.60	65.0	8.10	MoO_3	ZnO
	1.02	7.84%	PM6:ITIC	12.70	61.0	7.90	MoO_3	ZnO
127	1.03	8.74%	PM6:IT-M	12.81	67.9	8.86	PEDOT:PS	PDIN
	0.86	4.65%	PM6:Y6	24.77	70.7	14.8	PEDOT:PS	PDIN

128	1.03	8.74%	PM6:IT-M	15.65	64.6	10.3	PEDOT:PS	PDIN
129	0.80	12.07%	PM6:$Y6_{(CB)}$	23.09	69.9	12.9	PEDOT:PS	PDIN
	0.83	8.17%	PM6:$Y6_{(CF)}$	25.60	73.5	15.6	PEDOT:PS	PDIN
130	0.86	4.65%	PM6:Y6	24.30	73.2	15.3	PEDOT:PS	PDIN
131	0.85	5.63%	PM6:Y6	25.62	73.4	16.0	PEDOT:PS	PDIN

References:

[1] Guo, B., Yin, Q., Zhou, J., Li, W., Zhang, K., & Li, Y. Semiconductive polymer-doped PEDOT with high work function, conductivity, reversible dispersion, and application in organic solar cells. ACS Sustainable Chemistry & Engineering, 2019, 7(9), 8206-8214.

[2] Chen, X., Xu, G., Zeng, G., Gu, H., Chen, H., Xu, H., & Li, Y. Realizing ultrahigh mechanical flexibility and >15% efficiency of flexible organic solar cells via a “welding” flexible transparent electrode. Advanced Materials, 2020, 32(14), 1908478.

[3] Lu, L., Liao, Q., Zu, Y., Xu, Y., Xu, B., & Hou, J. Significant effect of fluorination on simultaneously improving work function and transparency of anode interlayer for organic solar cells. Advanced Energy Materials, 2019, 9(15), 1803826.

[4] Zeng, M., Wang, X., Ma, R., Zhu, W., Li, Y., Chen, Z., & Cao, Y. Dopamine semiquinone radical doped PEDOT: PSS: Enhanced conductivity, work function and performance in organic solar cells. Advanced Energy Materials, 2020, 10(25), 2000743.

[5] Mutlu, A., Can, M., & Tozlu, C. Performance improvement of organic solar cell via incorporation of donor type self-assembled interfacial monolayer. Thin Solid Films, 2019, 685, 88-96.

[6] Yao, J., Qiu, B., Zhang, Z. G., Xue, L., Wang, R., Zhang, C., & Li, Y. Cathode engineering with perylene-diimide interlayer enabling over 17% efficiency single-junction organic solar cells. Nature communications, 2020, 11(1), 1-10.

[7] Erray, M., Hanine, M., Boufounas, E. M., & El Amrani, A. Combined effects of carriers charge mobility and electrodes work function on the performances of polymer/fullerene P3HT: PCBM based organic photovoltaic solar cell. The European physical journal applied physics, 2018, 82(3), 30201.

[8] Cui, Y., Jia, G., Zhu, J., Kang, Q., Yao, H., Lu, L., & Hou, J. The critical role of anode work function in non-fullerene organic solar cells unveiled by counterion-size-controlled self-doping conjugated polymers. Chemistry of Materials, 2018, 30(3), 1078-1084.

[9] Xue, Z., Liu, X., Lv, Y., Zhang, N., & Guo, X. Low-work-function, ITO-free transparent cathodes for inverted polymer solar cells. ACS applied materials & interfaces, 2015, 7(36), 19960-19965.

[10] Cai, Y., Chang, L., You, L., Fan, B., Liu, H., & Sun, Y. Novel nonconjugated polymer as cathode buffer layer for efficient organic solar cells. ACS applied materials & interfaces, 2018, 10(28), 24082-24089.

[11] Tang, H., Feng, H., Wang, H., Wan, X., Liang, J., & Chen, Y. Highly conducting MXene–silver nanowire transparent electrodes for flexible organic solar cells. ACS applied materials & interfaces, 2019, 11(28), 25330-25337.

[12] Yu, Z., Li, B., & Ouyang, J. Metal ion/dendrimer complexes with tunable work functions in a wide range and their application as electron-and hole-transport materials of non-fullerene organic solar cells. Advanced Functional Materials, 2018, 28(33), 1802554.

[13] Song, W., Fan, X., Xu, B., Yan, F., Cui, H., Wei, Q., & Ge, Z. All-solution-processed metal-oxide-free flexible organic solar cells with over 10% efficiency. Advanced Materials, 2018, 30(26), 1800075.

[14] Jo, J. W., Jung, J. W., Bae, S., Ko, M. J., Kim, H., Jo, W. H., & Son, H. J. Development of Self-Doped Conjugated Polyelectrolytes with Controlled Work Functions and Application to Hole Transport Layer Materials for High-Performance Organic Solar Cells. Advanced Materials Interfaces, 2016, 3(12), 1500703.

[15] Wang, S., Li, Z., Xu, X., Zhang, G., Li, Y., & Peng, Q. Amino-functionalized graphene quantum dots as cathode interlayer for efficient organic solar cells: quantum dot size on interfacial modification ability and photovoltaic performance. Advanced Materials Interfaces, 2019, 6(3), 1801480.

[16] Zhao, C., Zhang, Z., Han, F., Xia, D., Xiao, C., Fang, J., & Li, W. An Organic-Inorganic Hybrid Electrolyte as a Cathode Interlayer for Efficient Organic Solar Cells. Angewandte Chemie, 2021, 133(15), 8607-8612.

[17] Cheng, J., Xie, F., Liu, Y., Wei, E. I., Li, X., Yang, Y., & Choy, W. C. Efficient hole transport layers with widely tunable work function for deep HOMO level organic solar cells. Journal of Materials Chemistry A, 2015, 3(47), 23955-23963.

[18] Borse, K., Sharma, R., Gupta, D., & Yella, A. Interface engineering through electron transport layer modification for high efficiency organic solar cells. RSC advances, 2018, 8(11), 5984-5991.

[19] Pan, F., Sun, C., Li, Y., Tang, D., Zou, Y., Li, X., & Li, Y. Solution-processable n-doped graphene-containing cathode interfacial materials for high-performance organic solar cells. Energy & Environmental Science, 2019, 12(11), 3400-3411.

[20] Jiang, Y., Sun, L., Jiang, F., Xie, C., Hu, L., Dong, X., & Zhou, Y. Photocatalytic effect of ZnO on the stability of nonfullerene acceptors and its mitigation by SnO2 for nonfullerene organic solar cells. Materials Horizons, 2019, 6(7), 1438-1443.

[21] Yu, Z., Feng, W., Lu, W., Li, B., Yao, H., Zeng, K., & Ouyang, J. MXenes with tunable work functions and their application as electron-and hole-transport materials in non-fullerene organic solar cells. Journal of Materials Chemistry A, 2019, 7(18), 11160-11169.

[22] Cheng, M., Xu, B., Chen, C., Yang, X., Zhang, F., Tan, Q., & Sun, L. Phenoxazine-based small molecule material for efficient perovskite solar cells and bulk heterojunction organic solar cells. Advanced Energy Materials, 2015, 5(8), 1401720.

[23] Wan, J., Fan, X., Huang, H., Wang, J., Zhang, Z., Fang, J., & Yan, F. Metal oxide-free flexible organic solar cells with 0.1 M perchloric acid sprayed polymeric anodes. Journal of Materials Chemistry A, 2020, 8(40), 21007-21015.

[24] Hsieh, Y. T., Chen, J. Y., Fukuta, S., Lin, P. C., Higashihara, T., Chueh, C. C., & Chen, W. C. Realization of intrinsically stretchable organic solar cells enabled by charge-extraction layer and photoactive material engineering. ACS applied materials & interfaces, 2018, 10(25), 21712-21720.

[25] Li, J., Wang, N., Wang, Y., Liang, Z., Peng, Y., Yang, C., & Xia, Y. Efficient inverted organic solar cells with a thin natural biomaterial L-Arginine as electron transport layer. Solar Energy, 2020, 196, 168-176.

[26] Chen, Y., Yue, Y. Y., Wang, S. R., Zhang, N., Feng, J., & Sun, H. B. Thermally-induced wrinkles on PH1000/graphene composite electrode for enhanced efficiency of organic solar cells. Solar Energy Materials and Solar Cells, 2019, 201, 110075.

[27] Jeon, I., Cui, K., Chiba, T., Anisimov, A., Nasibulin, A. G., Kauppinen, E. I., & Matsuo, Y. Direct and dry deposited single-walled carbon nanotube films doped with MoOx as electron-blocking transparent electrodes for flexible organic solar cells. Journal of the American Chemical Society, 2015, 137(25), 7982-7985.

[28] Kang, Q., Zheng, Z., Zu, Y., Liao, Q., Bi, P., Zhang, S., & Hou, J. n-doped inorganic molecular

clusters as a new type of hole transport material for efficient organic solar cells. Joule, 2021, 5(3), 646-658.

[29] Kim, H. J., Seo, K. W., Noh, Y. J., Na, S. I., Sohn, A., Kim, D. W., & Kim, H. K. Work function and interface control of amorphous IZO electrodes by MoO3 layer grading for organic solar cells. Solar Energy Materials and Solar Cells, 2015, 141, 194-202.

[30] Lee, B. H., Lee, J. H., Jeong, S. Y., Park, S. B., Lee, S. H., & Lee, K. Broad Work-Function Tunability of p-Type Conjugated Polyelectrolytes for Efficient Organic Solar Cells. Advanced Energy Materials, 2015, 5(5), 1401653.

[31] Liao, S. H., Jhuo, H. J., Cheng, Y. S., & Chen, S. A. Fullerene derivative-doped zinc oxide nanofilm as the cathode of inverted polymer solar cells with low-bandgap polymer (PTB7-Th) for high performance. Advanced materials, 2013, 25(34), 4766-4771.

[32] Lin, Y., Adilbekova, B., Firdaus, Y., Yengel, E., Faber, H., Sajjad, M., & Anthopoulos, T. D. 17% efficient organic solar cells based on liquid exfoliated WS2 as a replacement for PEDOT: PSS. Advanced materials, 2019, 31(46), 1902965.

[33] Lin, Y., Firdaus, Y., Isikgor, F. H., Nugraha, M. I., Yengel, E., Harrison, G. T., & Anthopoulos, T. D. Self-assembled monolayer enables hole transport layer-free organic solar cells with 18% efficiency and improved operational stability. ACS Energy Letters, 2020, 5(9), 2935-2944.

[34] Ma, R., Zeng, M., Li, Y., Liu, T., Luo, Z., Xu, Y., & Yan, H. Rational anode engineering enables progresses for different types of organic solar cells. Advanced Energy Materials, 2021, 11(23), 2100492.

[35] Sun, C., Wu, Z., Hu, Z., Xiao, J., Zhao, W., Li, H. W., & Cao, Y. Interface design for high-efficiency non-fullerene polymer solar cells. Energy & Environmental Science, 2017, 10(8), 1784-1791.

[36] Xing, W., Chen, Y., Wang, X., Lv, L., Ouyang, X., Ge, Z., & Huang, H. MoS2 quantum dots with a tunable work function for high-performance organic solar cells. ACS Applied Materials & Interfaces, 2016, 8(40), 26916-26923.

[37] Zhang, K., Xu, R., Ge, W., Qi, M., Zhang, G., Xu, Q. H., & Wang, X. Electrostatically self-assembled chitosan derivatives working as efficient cathode interlayers for organic solar cells. Nano Energy, 2017, 34, 164-171.

[38] Ding, Z., Hao, Z., Meng, B., Xie, Z., Liu, J., & Dai, L. Few-layered graphene quantum dots as efficient hole-extraction layer for high-performance polymer solar cells. Nano Energy, 2015, 15, 186-192.

[39] Konios, D., Kakavelakis, G., Petridis, C., Savva, K., Stratakis, E., & Kymakis, E. Highly efficient organic photovoltaic devices utilizing work-function tuned graphene oxide derivatives as the anode and cathode charge extraction layers. Journal of Materials Chemistry A, 2016, 4(5), 1612-1623.

[40] Lin, X., Yang, Y., Nian, L., Su, H., Ou, J., Yuan, Z., & Chen, X. Interfacial modification layers based on carbon dots for efficient inverted polymer solar cells exceeding 10% power conversion efficiency. Nano Energy, 2016, 26, 216-223.

[41] Liu, H., Hu, L., Wu, F., Chen, L., & Chen, Y. Polyfluorene electrolytes interfacial layer for efficient polymer solar cells: controllably interfacial dipoles by regulation of polar groups. ACS applied materials & interfaces, 2016, 8(15), 9821-9828.

[42] Wang, J., Zheng, Z., Zhang, D., Zhang, J., Zhou, J., Liu, J., & Zhou, H. Regulating

bulk-heterojunction molecular orientations through surface free energy control of hole-transporting layers for high-performance organic solar cells. Advanced Materials, 2019, 31(17), 1806921.
[43] Xu, B., Gopalan, S. A., Gopalan, A. I., Muthuchamy, N., Lee, K. P., Lee, J. S., & Kang, S. W. Functional solid additive modified PEDOT:PSS as an anode buffer layer for enhanced photovoltaic performance and stability in polymer solar cells. Scientific Reports, 2017, 7(1), 1-13.
[44] Zheng, Z., Hu, Q., Zhang, S., Zhang, D., Wang, J., Xie, S., & Zhou, H. A highly efficient non-fullerene organic solar cell with a fill factor over 0.80 enabled by a fine-tuned hole-transporting layer. Advanced materials, 2018, 30(34), 1801801.
[45] Zhang, L., Ding, Z. C., Tong, T., & Liu, J. Tuning the work functions of graphene quantum dot-modified electrodes for polymer solar cell applications. Nanoscale, 2017, 9(10), 3524-3529.
[46] Tran, H. N., Park, S., Wibowo, F. T. A., Krishna, N. V., Kang, J. H., Seo, J. H., & Cho, S. 17% Non-Fullerene Organic Solar Cells with Annealing-Free Aqueous MoOx. Advanced Science, 2020, 7(21), 2002395.
[47] Zhang, D., Wang, J., Zhang, X., Zhou, J., Zafar, S. U., Zhou, H., & Zhang, Y. Sequential molecular doping of non-fullerene organic solar cells without hole transport layers. Journal of Materials Chemistry C, 2020, 8(1), 158-164.
[48] Babu, B. H., Lyu, C., Zhang, H., Chen, Z., Li, F., Feng, L., & Hao, X. T. Modification of Hole Transport Layers for Fabricating High Performance Non-fullerene Polymer Solar Cells. Chinese Journal of Chemistry, 2020, 38(8), 817-822.
[49] Hou, C., & Yu, H. Modifying the nanostructures of PEDOT:PSS/Ti3C2TX composite hole transport layers for highly efficient polymer solar cells. Journal of Materials Chemistry C, 2020, 8(12), 4169-4180.
[50] Hilal, M., & Han, J. I. Significant improvement in the photovoltaic stability of bulk heterojunction organic solar cells by the molecular level interaction of graphene oxide with a PEDOT:PSS composite hole transport layer. Solar Energy, 2018, 167, 24-34.
[51] Li, W., Cai, J., Yan, Y., Cai, F., Li, S., Gurney, R. S., & Wang, T. Correlating Three-dimensional Morphology With Function in PBDB-T: IT-M Non-Fullerene Organic Solar Cells. Solar RRL, 2018, 2(9), 1800114.
[52] Nicasio-Collazo, J., Maldonado, J. L., Salinas-Cruz, J., Barreiro-Argüelles, D., Caballero-Quintana, I., Vazquez-Espinosa, C., & Romero-Borja, D. Functionalized and reduced graphene oxide as hole transport layer and for use in ternary organic solar cell. Optical Materials, 2019, 98, 109434.
[53] Zheng, X., Zhang, H., Yang, Q., Xiong, C., Li, W., Yan, Y., & Wang, T. Solution-processed Graphene-MoS2 heterostructure for efficient hole extraction in organic solar cells. Carbon, 2019, 142, 156-163.
[54] Tang, H., Liu, Z., Hu, Z., Liang, Y., Huang, F., & Cao, Y. Oxoammonium enabled secondary doping of hole transporting material PEDOT:PSS for high-performance organic solar cells. Science China Chemistry, 2020, 63(6), 802-809.
[55] Kang, Q., Zu, Y., Liao, Q., Zheng, Z., Yao, H., Zhang, S., & Hou, J. An inorganic molecule-induced electron transfer complex for highly efficient organic solar cells. Journal of Materials Chemistry A, 2020, 8(11), 5580-5586.

[56] Soultati, A., Verykios, A., Panagiotakis, S., Armadorou, K. K., Haider, M. I., Kaltzoglou, A., & Vasilopoulou, M. Suppressing the photocatalytic activity of zinc oxide electron-transport layer in nonfullerene organic solar cells with a pyrene-bodipy interlayer. ACS applied materials & interfaces, 2020, 12(19), 21961-21973.
[57] Huai, Z., Wang, L., Sun, Y., Fan, R., Huang, S., Zhao, X., & Yang, S. High-efficiency and stable organic solar cells enabled by dual cathode buffer layers. ACS applied materials & interfaces, 2018, 10(6), 5682-5692.
[58] Chen, S., Wang, Y., Zhang, L., Zhao, J., Chen, Y., Zhu, D., & Yan, H. Efficient nonfullerene organic solar cells with small driving forces for both hole and electron transfer. Advanced Materials, 2018, 30(45), 1804215.
[59] Yin, Z., Zheng, Q., Chen, S. C., Cai, D., & Ma, Y. Controllable ZnMgO Electron-Transporting Layers for Long-Term Stable Organic Solar Cells with 8.06% Efficiency after One-Year Storage. Advanced Energy Materials, 2016, 6(4), 1501493.
[60] Wang, Z., Zheng, N., Zhang, W., Yan, H., Xie, Z., Ma, Y., & Cao, Y. Self-Doped, n-Type Perylene Diimide Derivatives as Electron Transporting Layers for High-Efficiency Polymer Solar Cells. Advanced Energy Materials, 2017, 7(15), 1700232.
[61] Lee, E. J., Heo, S. W., Han, Y. W., & Moon, D. K. An organic-inorganic hybrid interlayer for improved electron extraction in inverted polymer solar cells. Journal of Materials Chemistry C, 2016, 4(13), 2463-2469.
[62] Zhu, L., Lu, Q., Lv, L., Wang, Y., Hu, Y., Deng, Z., & Teng, F. Ligand-free rutile and anatase TiO2 nanocrystals as electron extraction layers for high performance inverted polymer solar cells. RSC advances, 2017, 7(33), 20084-20092.
[63] Borse, K., Sharma, R., Gupta, D., & Yella, A. Interface engineering through electron transport layer modification for high efficiency organic solar cells. RSC advances, 2018, 8(11), 5984-5991.
[64] Zheng, Z., Zhang, S., Wang, J., Zhang, J., Zhang, D., Zhang, Y., & Zhou, H. Exquisite modulation of ZnO nanoparticle electron transporting layer for high-performance fullerene-free organic solar cell with inverted structure. Journal of Materials Chemistry A, 2019, 7(8), 3570-3576.
[65] Ling, Z., Zhao, Y., Wang, S., Pan, S., Lian, H., Peng, C., & Chen, G. High-performance light-soaking-free polymer solar cells based on a LiF modified ZnO electron extraction layer. Journal of Materials Chemistry C, 2019, 7(30), 9354-9361.
[66] Wang, Y., Liang, Z., Li, X., Qin, J., Ren, M., Yang, C., & Li, J. Self-doping n-type polymer as a cathode interface layer enables efficient organic solar cells by increasing built-in electric field and boosting interface contact. Journal of Materials Chemistry C, 2019, 7(36), 11152-11159.
[67] Tran, V. H., Eom, S. H., Yoon, S. C., Kim, S. K., & Lee, S. H. Enhancing device performance of inverted organic solar cells with SnO2/Cs2CO3 as dual electron transport layers. Organic Electronics, 2019, 68, 85-95.
[68] Wei, J., Zhang, C., Ji, G., Han, Y., Ismail, I., Li, H., & Ma, C. Q. Roll-to-roll printed stable and thickness-independent ZnO:PEI composite electron transport layer for inverted organic solar cells. Solar Energy, 2019, 193, 102-110.
[69] Upama, M. B., Elumalai, N. K., Mahmud, M. A., Xu, C., Wang, D., Wright, M., & Uddin, A. Enhanced electron transport enables over 12% efficiency by interface engineering of non-

fullerene organic solar cells. Solar Energy Materials and Solar Cells, 2018, 187, 273-282.
[70] Tountas, M., Topal, Y., Polydorou, E., Soultati, A., Verykios, A., Kaltzoglou, A., & Vasilopoulou, M. Low work function lacunary polyoxometalates as electron transport interlayers for inverted polymer solar cells of improved efficiency and stability. ACS Applied Materials & Interfaces, 2017, 9(27), 22773-22787.
[71] Hu, H. C., Xu, H., Wu, J., Li, L., Yue, F., Huang, L., & Ouyang, X. Secondary Bonds Modifying Conjugate-Blocked Linkages of Biomass-Derived Lignin to Form Electron Transfer 3D Networks for Efficiency Exceeding 16% Nonfullerene Organic Solar Cells. Advanced Functional Materials, 2020, 30(23), 2001494.
[72] Yao, J., Qiu, B., Zhang, Z. G., Xue, L., Wang, R., Zhang, C., & Li, Y. Cathode engineering with perylene-diimide interlayer enabling over 17% efficiency single-junction organic solar cells. Nature communications, 2020, 11(1), 1-10.
[73] Kadam, K. D., Kim, H., Rehman, S., Patil, H., Aziz, J., Dongale, T. D., & Kim, D. K. Optimization of ZnO:PEIE as an electron transport layer for flexible organic solar cells. Energy & Fuels, 2021, 35(15), 12416-12424.
[74] Yan, Y., Cai, F., Yang, L., Li, J., Zhang, Y., Qin, F., & Wang, T. Light-Soaking-Free Inverted Polymer Solar Cells with an Efficiency of 10.5% by Compositional and Surface Modifications to a Low-Temperature-Processed TiO2 Electron-Transport Layer. Advanced Materials, 2017, 29(1), 1604044.
[75] Huang, X., Yu, H., Shi, S., & Huang, C. Improving the performance of inverted polymer solar cells by the efficiently doping and modification of electron transport layer-ZnO. Organic Electronics, 2019, 65, 311-320.
[76] Qiu, B., Chen, S., Li, H., Luo, Z., Yao, J., Sun, C., & Li, Y. A simple approach to prepare chlorinated polymer donors with low-lying HOMO level for high performance polymer solar cells. Chemistry of Materials, 2019, 31(17), 6558-6567.
[77] Zhao, F., Deng, L., Wang, K., Han, C., Liu, Z., Yu, H., & Hu, B. Surface modification of SnO2 via MAPbI3 nanowires for a highly efficient non-fullerene acceptor-based organic solar cell. ACS applied materials & interfaces, 2020, 12(4), 5120-5127.
[78] Lei, T., Peng, R., Huang, L., Song, W., Yan, T., Zhu, L., & Ge, Z. 13.5% flexible organic solar cells achieved by robust composite ITO/PEDOT:PSS electrodes. Materials Today Energy, 2019, 14, 100334.
[79] Wang, Y., Li, N., Cui, M., Li, Y., Tian, X., Xu, X., & Nian, L. High-performance hole transport layer based on WS2 doped PEDOT:PSS for organic solar cells. Organic Electronics, 2021, 99, 106305.
[80] Zhang, X., Zhang, B., Ouyang, X., Chen, L., & Wu, H. Polymer solar cells employing water-soluble polypyrrole nanoparticles as dopants of PEDOT:PSS with enhanced efficiency and stability. The Journal of Physical Chemistry C, 2017, 121(34), 18378-18384.
[81] Wang, J., Yu, H., Hou, C., & Zhang, J. Solution-processable PEDOT:PSS: α-In2Se3 with enhanced conductivity as a hole transport layer for high-performance polymer solar cells. ACS applied materials & interfaces, 2020, 12(23), 26543-26554.
[82] Xu, R., Zhang, K., Liu, X., Jin, Y., Jiang, X. F., Xu, Q. H., & Cao, Y. Alkali salt-doped highly transparent and thickness-insensitive electron-transport layer for high-performance polymer solar cell. ACS applied materials & interfaces, 2018, 10(2), 1939-1947.

[83] Gupta, M., Yan, D., Xu, J., Yao, J., & Zhan, C. Tetraphenylphosphonium bromide as a cathode buffer layer material for highly efficient polymer solar cells. ACS applied materials & interfaces, 2018, 10(6), 5569-5576.
[84] Zhang, J., Xue, R., Xu, G., Chen, W., Bian, G. Q., Wei, C., & Li, Y. Self-Doping Fullerene Electrolyte-Based Electron Transport Layer for All-Room-Temperature-Processed High-Performance Flexible Polymer Solar Cells. Advanced Functional Materials, 2018, 28(13), 1705847.
[85] Huang, J., Yu, H., & Zhou, X. ZnO nanoparticles modified with biomaterial GHK-Cu as electron transport layer to fabricate highly efficient inverted polymer solar cells. Chemical Engineering Journal, 2022, 428, 131366.
[86] Cheng, J., Zhang, H., Zhao, Y., Mao, J., Li, C., Zhang, S., & Choy, W. C. Self-Assembled Quasi-3D Nanocomposite: A Novel p-Type Hole Transport Layer for High Performance Inverted Organic Solar Cells. Advanced Functional Materials, 2018, 28(15), 1706403.
[87] Gao, X., Su, Z., Qu, S., Zhang, W., Gao, Y., He, S., & Wang, Z. Efficient and moisture-resistant organic solar cells via simultaneously reducing the surface defects and hydrophilicity of an electron transport layer. Journal of Materials Chemistry C, 2021, 9(38), 13500-13508.
[88] Liu, L., Li, F., Zhao, C., Bi, F., Jiu, T., Zhao, M., & Xiao, X. Performance enhancement of conventional polymer solar cells with TTF-py-modified PEDOT:PSS film as the hole transport layer. ACS Applied Energy Materials, 2019, 2(9), 6577-6583.
[89] Wang, Y., Li, J., Li, T., Wang, J., Liu, K., Jiang, Q., & Zhan, X. Black phosphorous quantum dots sandwiched organic solar cells. Small, 2019, 15(47), 1903977.
[90] Liu, L., Zhou, S., Zhao, C., Jiu, T., Bi, F., Jian, H., & Xiao, X. TTA as a potential hole transport layer for application in conventional polymer solar cells. Journal of Energy Chemistry, 2020, 42, 210-216.
[91] Zhao, W., Yan, L., Gu, H., Li, Z., Wang, Y., Luo, Q., & Ma, C. Q. Zinc oxide coated carbon dot nanoparticles as electron transport layer for inverted polymer solar cells. ACS Applied Energy Materials, 2020, 3(11), 11388-11397.
[92] Liu, H., Ma, Z., Yu, R., Gao, H., Lin, J., Hayat, T., & Tan, Z. A. Crosslinkable metal chelate as the electron transport layer for efficient and stable inverted polymer solar cells. Materials Chemistry Frontiers, 2020, 4(10), 2995-3002.
[93] Aatif, M., & Tiwari, J. P. Futuristic electron transport layer based on multifunctional interactions of ZnO/TCNE for stable inverted organic solar cells. RSC advances, 2020, 10(69), 42305-42317.
[94] Hou, C., Yu, H., & Huang, C. Solution-processable Ti3C2Tx nanosheets as an efficient hole transport layer for high-performance and stable polymer solar cells. Journal of Materials Chemistry C, 2019, 7(37), 11549-11558.
[95] Hong, J., Zhang, D., Kwon, H. J., Park, C. E., Kwon, S. K., & Kim, Y. H. A Solution-Processed Cathode Interfacial Layer Facilitates Efficient Energy Level Alignment in Organic Photovoltaics. The Journal of Physical Chemistry C, 2021, 125(36), 20067-20075.
[96] Li, Y., Han, M., Yang, W., Guo, J., Chang, K., Wang, J., & Li, Z. Perylene diimide-based cathode interfacial materials: adjustable molecular structures and conformation, optimized film morphology, and much improved performance of non-fullerene polymer solar cells. Materials Chemistry Frontiers, 2019, 3(9), 1840-1848.
[97] Lin, L., Huang, Z., Luo, Y., Peng, T., He, B., Chen, G., & Yang, W. Alcohol-soluble fluorene

derivate functionalized with pyridyl groups as a high-performance cathode interfacial material in organic solar cells. New Journal of Chemistry, 2021, 45(10), 4584-4591.
[98] Chen, G., Qian, G., Yi, S., He, Z., Wu, H. B., Yang, W., & Cao, Y. Molecular Engineering on Bis (benzothiophene-S, S-dioxide)-Based Large-Band Gap Polymers for Interfacial Modifications in Polymer Solar Cells. ACS applied materials & interfaces, 2019, 11(49), 45969-45978.
[99] Prasetio, A., Jahandar, M., Kim, S., Heo, J., Kim, Y. H., & Lim, D. C. Mitigating the Undesirable Chemical Reaction between Organic Molecules for Highly Efficient Flexible Organic Photovoltaics. Advanced Science, 2021, 8(14), 2100865.
[100] Kim, S., Prasetio, A., Han, J. W., Kim, Y., Shin, M., Heo, J., & Lim, D. C. Enhanced flexible optoelectronic devices by controlling the wettability of an organic bifacial interlayer. Communications Materials, 2021, 2(1), 1-10.
[101] Li, J., Qin, F., Zeng, W., Sun, L., Wang, W., & Zhou, Y. N-doping of fullerene using 1,3,5-trimethylhexahydro-1,3,5-triazine as an electron transport layer for nonfullerene organic solar cells. Sustainable Energy & Fuels, 2020, 4(4), 1984-1990.
[102] Wang, Z., Dong, J., Guo, J., Wang, Z., Yan, L., Hao, Y., & Yin, S. Hybrid Hole Extraction Layer Enabled High Efficiency in Polymer Solar Cells. ACS Applied Materials & Interfaces, 2020, 12(49), 55342-55348.
[103] Lu, L., Kang, Q., Yang, C., Xu, B., & Hou, J. Conjugated polymers containing sulfonic acid fluorene unit for achieving multiple interfacial modifications in fullerene-free organic solar cells. The Journal of Physical Chemistry C, 2018, 122(34), 19328-19337.
[104] Soultati, A., Fakharuddin, A., Polydorou, E., Drivas, C., Kaltzoglou, A., Haider, M. I., & Vasilopoulou, M. Lithium doping of ZnO for high efficiency and stability fullerene and non-fullerene organic solar cells. ACS Applied Energy Materials, 2019, 2(3), 1663-1675.
[105] Chen, H., Liu, L., Zhao, M., Zhang, G. H., Zhao, C., Jiu, T., & Tao, G. H. Interfacial Carrier-Transfer Channel Optimization Based on Hydrogen Bonds for High-Performance Organic Solar Cells. ACS Applied Energy Materials, 2021, 4(4), 3881-3890.
[106] Gao, J., Ge, J., Peng, R., Liu, C., Cao, L., Zhang, D., & Ge, Z. Over 14% efficiency nonfullerene all-small-molecule organic solar cells enabled by improving the ordering of molecular donors via side-chain engineering. Journal of materials chemistry A, 2020, 8(15), 7405-7411.
[107] Yu, Y., Tan, X., Ning, S., & Wu, Y. Machine learning for understanding compatibility of organic-inorganic hybrid perovskites with post-treatment amines. ACS Energy Letters, 2019, 4(2), 397-404.
[108] Bhavani, T. T., Rao, M. K., & Reddy, A. M. Network intrusion detection system using random forest and decision tree machine learning techniques. First international conference on sustainable technologies for computational intelligence. Springer, Singapore, 2020, (pp. 637-643).
[109] Lee, M. H. Machine Learning for Understanding the Relationship between the Charge Transport Mobility and Electronic Energy Levels for n-Type Organic Field-Effect Transistors. Advanced Electronic Materials, 2019, 5(12), 1900573.
[110] Chen, T., & Guestrin, C. Xgboost: A scalable tree boosting system. In Proceedings of the 22nd acm sigkdd international conference on knowledge discovery and data mining. 2016, (pp. 785-794).

[111] Hao, T., Leng, S., Yang, Y., Zhong, W., Zhang, M., Zhu, L., ... & Liu, F. Capture the high-efficiency non-fullerene ternary organic solar cells formula by machine-learning-assisted energy-level alignment optimization. Patterns, 2021, 2(9), 100333.
[112] Cai, Y., Chang, L., You, L., Fan, B., Liu, H., & Sun, Y. Novel nonconjugated polymer as cathode buffer layer for efficient organic solar cells. ACS applied materials & interfaces, 2018, 10(28), 24082-24089.
[113] Singh, R., Suranagi, S. R., Lee, J., Lee, H., Kim, M., & Cho, K. Unraveling the efficiency-limiting morphological issues of the perylene diimide-based non-fullerene organic solar cells. Scientific Reports, 2018, 8(1), 1-9.
[114] Wang, Z., Dong, J., Guo, J., Wang, Z., Yan, L., Hao, Y., ... & Yin, S. Hybrid Hole Extraction Layer Enabled High Efficiency in Polymer Solar Cells. ACS Applied Materials & Interfaces, 2020, 12(49), 55342-55348.
[115] Sharma, G. D., Bucher, L., Desbois, N., Gros, C. P., Gupta, G., & Malhotra, P. Polymer solar cell based on ternary active layer consists of medium bandgap polymer and two non-fullerene acceptors. Solar Energy, 2020, 207, 1427-1433.
[116] Gao, J., Ge, J., Peng, R., Liu, C., Cao, L., Zhang, D., ... & Ge, Z. Over 14% efficiency nonfullerene all-small-molecule organic solar cells enabled by improving the ordering of molecular donors via side-chain engineering. Journal of materials chemistry A, 2020, 8(15), 7405-7411.
[117] Wang, S., Li, Z., Xu, X., Zhang, G., Li, Y., & Peng, Q. Amino-functionalized graphene quantum dots as cathode interlayer for efficient organic solar cells: quantum dot size on interfacial modification ability and photovoltaic performance. Advanced Materials Interfaces, 2019, 6(3), 1801480.
[118] Wang, J., Tong, Y., Zhang, X., Li, Z., Hao, Y., & Wang, H. PTB7: PC71BM bulk heterojunction solar cells exhibiting 9.64% efficiency via adopting moderate polarity solvent vapor annealing treatment. Molecular Crystals and Liquid Crystals, 2022, 740(1), 127-137.
[119] Kim, W., Choi, J., Kim, J. H., Kim, T., Lee, C., Lee, S., ... & Kim, T. S. Comparative Study of the mechanical properties of all-polymer and fullerene-polymer solar cells: the importance of polymer acceptors for high fracture resistance. Chemistry of Materials, 2018, 30(6), 2102-2111.
[120] Song, L., Wang, W., Barabino, E., Yang, D., Körstgens, V., Zhang, P., ... & Müller-Buschbaum, P. Composition-morphology correlation in PTB7-Th/PC71BM blend films for organic solar cells. ACS applied materials & interfaces, 2018, 11(3), 3125-3135.
[121] Lu, W., Peng, Y., Chen, Q., Tang, W., Pang, T., Zhang, S., ... & Wang, X. Hole transport layer free bulk heterojunction organic solar cells with high work function ITO anodes. AIP Advances, 2018, 8(9), 095027.
[122] Zhao, J., Zhao, S., Xu, Z., Qiao, B., Huang, D., Zhao, L., ... & Wang, P. Revealing the effect of additives with different solubility on the morphology and the donor crystalline structures of organic solar cells. ACS Applied Materials & Interfaces, 2016, 8(28), 18231-18237.
[123] Zheng, Y., Wang, G., Huang, D., Kong, J., Goh, T., Huang, W., ... & Taylor, A. D. Binary solvent additives treatment boosts the efficiency of PTB7: PCBM polymer solar cells to over 9.5%. Solar Rrl, 2018, 2(4), 1700144.
[124] Sharma, R., Gupta, V., Lee, H., Borse, K., Datt, R., Sharma, C., ... & Gupta, D. Charge carrier dynamics in PffBT4T-2OD: PCBM organic solar cells. Organic Electronics, 2018, 62, 441-447.

[125] Kim, G. U., Lee, Y. W., Ma, B. S., Kim, J., Park, J. S., Lee, S., ... & Kim, B. J. Triad-type, multi-functional compatibilizers for enhancing efficiency, stability and mechanical robustness of polymer solar cells. Journal of Materials Chemistry A, 2020, 8(27), 13522-13531.
[126] Jain, N., Sharma, R., Mahesh, S., Moghe, D., Snaith, H. J., Yoo, S., & Kabra, D. Role of Electronic States and Their Coupling on Radiative Losses of Open-Circuit Voltage in Organic Photovoltaics. ACS Applied Materials & Interfaces, 2021, 13(50), 60279-60287.
[127] Wang, X., Zhai, X., Jing, X., Gao, C., He, Y., Yu, L., & Sun, M. Incorporation of a classical visible non-fullerene acceptor into host binary blend enable ternary high-performance semitransparent polymer solar cells. Chemical Engineering Journal, 2022, 427, 132048.
[128] Gao, J., Ma, X., Xu, C., Wang, X., Son, J. H., Jeong, S. Y., ... & Zhang, F. Over 17.7% efficiency ternary-blend organic solar cells with low energy-loss and good thickness-tolerance. Chemical Engineering Journal, 2022, 428, 129276.
[129] Fan, H., Yang, H., Wu, Y., Yildiz, O., Zhu, X., Marszalek, T., ... & Li, Y. Anthracene-Assisted Morphology Optimization in Photoactive Layer for High-Efficiency Polymer Solar Cells. Advanced Functional Materials, 2021, 31(37), 2103944.
[130] Yuan, J., Zhang, Y., Zhou, L., Zhang, G., Yip, H. L., Lau, T. K., ... & Zou, Y. Single-junction organic solar cell with over 15% efficiency using fused-ring acceptor with electron-deficient core. Joule, 2019, 3(4), 1140-1151.
[131] Deng, J., Huang, B., Li, W., Zhang, L., Jeong, S. Y., Huang, S., ... & Chen, L. Ferroelectric Polymer Drives Performance Enhancement of Non-fullerene Organic Solar Cells. Angewandte Chemie International Edition, 2022, 61(25), e202202177.